The Dissertation Committee for Peijia Liu
certifies that this is the approved version of the following dissertation:

Approximation of the 2D Complex Eikonal Equation: Analysis and Simulation

Committee:

Bjorn Engquist, Supervisor

Yen-Hsi Tsai

Irene Gamba

Alexis Vasseur

Omar Ghattas

Approximation of the 2D Complex Eikonal Equation: Analysis and Simulation

by

Peijia Liu, B.S.

DISSERTATION

Presented to the Faculty of the Graduate School of

The University of Texas at Austin

in Partial Fulfillment

of the Requirements

for the Degree of

DOCTOR OF PHILOSOPHY

THE UNIVERSITY OF TEXAS AT AUSTIN

December 2012

For my parents who always knew I could,

for their unconditional love, support, care, and understanding

and

Dedicated to the memory of my grandfather,

who I am always missing

Acknowledgments

I would like to thank my advisor Dr. Engquist for his generosity and guidance throughout these past few years. He has been immensely kind and willing to give his time. I have been truly honored to work with him.

Approximation of the 2D Complex Eikonal Equation: Analysis and Simulation

Publication No. ____________________

Peijia Liu, Ph.D.
The University of Texas at Austin, 2012

Supervisor: Bjorn Engquist

High frequency wave propagation is well described even at caustics by Gaussian beams and the complex eikonal equation. In contrast to the real eikonal equation, the complex eikonal equation is elliptic and not well posed as an initial value problem. We develop a new model that approximates the 2D complex eikonal equation but is well posed as an initial value problem. This model consists of a coupled system of partial and ordinary differential equations. We prove that there exists a local solution to this new system by a Picard iteration method and show uniqueness under certain constraints. Different numerical approximations are then developed based on direct finite difference approximations or the method of characteristics. Numerical simulations with a variety of velocity profiles are presented and compared with solutions to the corresponding Helmholtz equation.

Table of Contents

Chapter 1

Introduction

Classical ray theory gives an asymptotic approximation of the high frequency wave propagation with numerous applications in such fields as acoustics, electromagnetic, optics and geophysics. Its fundamental idea is to evaluate the wave field along the characteristic curves known as *Rays* in terms of a traveltime and amplitude that propagates along the ray. Here we would like to briefly review some key facts about classical ray theory. There are some notations and equations in classical ray theory we will use later to establish our model. Throughout this thesis, all of our discussions are in the two-dimensional plane $\mathbb{R}^2$.

Assume the wave is harmonic in time and consider the Helmholtz equation

$$\Delta U(x, y) + \frac{\omega^2}{c^2} U(x, y) = 0$$

where Δ is the Laplace operator, ω is the circular frequency and $c(x, y)$ is the velocity. By substituting the following asymptotic series of $U(x, y)$

$$U \sim e^{i\omega\tau} \sum_{j=0}^{\infty} \frac{A_j(x, y)}{(i\omega)^j}$$

into the Helmholtz equation and setting the coefficients of the terms $(i\omega)^2$ and

$i\omega$ to zero, we obtain the eikonal equation

$$\tau_x^2 + \tau_y^2 = \frac{1}{c^2(x,y)} \tag{1.1}$$

and the transport equation

$$2\nabla\tau \cdot \nabla A + A\Delta\tau = 0. \tag{1.2}$$

where we use the notation A to replace A_0.

There are several ways to solve the eikonal equation (1.1), such as the Hamiltonian approach and the method of characteristics. Here we endorse the later means. Suppose there is a ray $(x(s), y(s))$ in $\mathbb{R}^2$ where s is the arc length. Along this curve, we define functions $z(s) = \tau(x(s), y(s))$, $p_1(s) = \tau_x(x(s), y(s))$, $p_2(s) = \tau_y(x(s), y(s))$ and $\mathbf{c} = c(x(s), y(s))$. The functions x, y, z, p_1 and p_2 are determined by the following system of equations

$$x_s = \mathbf{c}p_1,\ y_s = \mathbf{c}p_2,\ {p_1}_s = (\frac{1}{\mathbf{c}})_x,\ {p_2}_s = (\frac{1}{\mathbf{c}})_y,\ z_s = \frac{1}{\mathbf{c}}$$

from which, we can derive two important facts about the eikonal τ: (a) τ represents the traveltime along the ray; (b) $\nabla\tau$ is tangent to the ray.

To solve the transport equation (1.2), we have to first introduce another coordinate system (θ, τ) where θ is a parameter labeling the ray. Then the amplitude $A(\theta, \tau)$ is solved as

$$A(\theta,\tau) = \text{constant}\sqrt{\frac{c}{J}} \ \text{ with } J = \left|\frac{D(x,y)}{D(\theta,\tau)}\right|$$

where $\left|\frac{D(x,y)}{D(\theta,\tau)}\right|$ is the Jacobian between coordinate systems (θ, τ) and (x, y).

Suppose a group of rays has an envelope line γ and this envelope line is called *caustic* in classical ray theory. In other words, *caustic* is a curve that each ray from this group is tangent to. We will show that J is zero at caustic. For any point on γ, there exists a ray touching γ at this point. Thus we can assume that γ is a function of θ such that $\gamma(\theta) = \vec{r}(\theta, \tau(\theta))$ where $\vec{r}(\theta, \tau) = (x(\theta, \tau), y(\theta, \tau))$. It's easy to see that γ_θ is parallel to $\vec{r}_\tau$ on γ. Since $\gamma_\theta = \vec{r}_\theta + \vec{r}_\tau \tau'(\theta)$, then $\vec{r}_\theta$ is parallel to $\vec{r}_\tau$ on γ. Therefore $J = |\vec{r}_\theta \times \vec{r}_\tau| = 0$ on γ. It means that classical ray theory fails in the computation of amplitude at caustic.

Indeed, the caustic problem is a major drawback of classical ray theory. In 1982, M.M. Popov introduced Gaussian beams to overcome this difficulty by adding a complex correction term to the eikonal [26]. Each Gaussian beam is an asymptotic solution of the wave equation in the vicinity of its central ray. We will first show the derivation of Gaussian beams in 2D and then talk about how to use Gaussian beams to evaluate the wave field, the approach known as the Gaussian beam method.

The derivation is based on the ray centered coordinates (s, n) in the vicinity of a ray where s is the arc length along the central ray and n is the measure along the normal direction off the central ray. Assuming n is small, we express the eikonal $\phi(s, n)$ as a power series in n with a collection of the first three terms

$$\phi(s, n) \approx \phi_0(s) + \phi_1(s)n + \frac{1}{2}\phi_2(s)n^2$$

where $\phi_0(s) = \phi(s,0)$, $\phi_1(s) = \dfrac{\partial}{\partial n}\phi(s,0)$ and $\phi_2(s) = \dfrac{\partial^2}{\partial n^2}\phi(s,0)$. Since $\nabla\phi$ is tangent to the central ray, $\phi_1 = 0$. Hence the eikonal $\phi(s,n)$ is reduced to

$$\phi(s,n) \approx \phi_0(s) + \frac{1}{2}\phi_2(s)n^2. \tag{1.3}$$

In the ray centered coordinates (s,n), the 2D eikonal equation is expressed as

$$\frac{1}{h^2}\left(\frac{\partial\phi}{\partial s}\right)^2 + \left(\frac{\partial\phi}{\partial n}\right)^2 = \frac{1}{c^2(s,n)} \tag{1.4}$$

where $h = 1 - k(s)n$ and $k(s)$ is the curvature of the ray. We substitute (1.3) into (1.4), express $\dfrac{1}{h^2}$ and $\dfrac{1}{c^2}$ as a power series in n, and collect the coefficients of the first and second order terms respectively to derive the equations for ϕ_0 and ϕ_2:

$$\phi_0'(s) = \frac{1}{c(s,0)} \implies \phi_0(s) = \int_0^s \frac{d\tau}{c(\tau,0)}$$

and

$$\frac{d}{ds}\phi_2(s) + c(s,0)\phi_2^2(s) + \frac{c_{nn}(s,0)}{c^2(s,0)} = 0. \tag{1.5}$$

Noting (1.5) is a Ricatti equation, we assume

$$\phi_2(s) = \frac{P(s)}{Q(s)}.$$

Substituting it into (1.5), then P, Q are subject to

$$\frac{dQ}{ds} = c(s,0)P, \quad \frac{dP}{ds} = -\frac{c_{nn}(s,0)}{c^2(s,0)}Q.$$

The amplitude function can also be expressed as a power series in n along the central ray. Here we only consider seeking its zero order term $A_0 = A(s,0)$, the amplitude along the central ray. For neatness, we replace the notation $A_0(s)$

with $A(s)$. From the transport equation in the ray centered coordinates, we can extract the following equation for A

$$\frac{2}{c(s,0)}\frac{dA}{ds}+A(\frac{d^2\phi_0}{ds^2}+\phi_2)=0$$

which is equivalent to

$$\frac{2}{c(s,0)}\frac{dA}{ds}+A\frac{d}{ds}(\frac{1}{c(s,0)})+A\frac{P}{Q}=0.$$

This can be transformed into

$$\frac{d}{ds}(\frac{A^2}{c(s,0)})+A^2\frac{Q'}{c(s,0)Q}=0$$

which leads to

$$\frac{d}{ds}(\frac{A^2Q}{c(s,0)})=0.$$

Clearly,

$$A(s)=\text{constant}\sqrt{\frac{c(s,0)}{Q}}.$$

Thus Gaussian beams denoted by u_{GB} have the following expression

$$u_{GB}=\text{constant}\sqrt{\frac{c(s,0)}{Q}}\exp(\,i\omega\int_0^s\frac{d\tau}{c(\tau,0)}+\frac{i\omega}{2}\frac{P(s)}{Q(s)}n^2).$$

Moreover, the selected complex-valued initial conditions for P and Q will guarantee that

$$(a)\;\; Q\neq 0 \;\text{ and }\; (b)\;\; \mathrm{Im}(\frac{P}{Q})>0 \;\text{ hold everywhere.}$$

The condition (a) will prevent the amplitude from becoming infinity at caustics. The condition (b) will have Gaussian beams decay exponentially in the normal direction from the central ray and will make Gaussian beams have significant amplitude only in a close tube around the central ray. The arguments for (a) can be found in [14] and (b) in [6, Section 3.2.1]. Finally, we would like to give an example of a Gaussian beam in the homogeneous medium with $c(x,y)=1$. With the initial conditions $Q(0)=1$ and $P(0)=i$

$$u_{GB}(x,y)=\sqrt{\frac{1}{1+iy}}\exp(-\omega\frac{x^2}{2(1+y^2)})\exp(i\omega(\,y+\frac{yx^2}{2(1+y^2)}))$$

whose amplitude has a Gaussian profile $e^{-\frac{x^2}{2}}$ on the x-axis at the initial time.

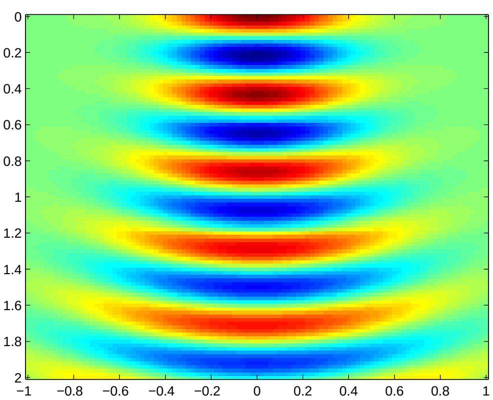

Figure 1.1: An imagesc picture of the real part of u_{GB}

The Gaussian beam method is a powerful tool for the computation of high frequency wave fields. Its evaluation of the wave field at certain point, say D, is the superposition of all the Gaussian beams whose amplitudes are not vanishing at D. The advantages of this method include: (1) It can be applied to complex velocity structures with no singularities at caustics. (2) Its representation of the wave field at D depends on the nearby area of D.

The Gaussian beam method was first proposed by Popov in [26] and its first application was introduced by Červený, Popov and Pšenčik in [12]. More details and applications can be found in the review [1] and in the books [9], [27] and [6].

From what we have reviewed of Gaussian beams, the complex eikonal holds clear advantages over the real eikonal from classical ray theory. This motivates us to explore a new approach to calculate the complex eikonal in a more global setting other than obtaining it by computing the second order derivative with respect to n along each ray from a fan of rays which are dense enough to cover the velocity structure. We consider solving the 2D complex eikonal equation

$$a_x^2 + a_y^2 - b_x^2 - b_y^2 - \frac{1}{c^2} = 0 \tag{1.6}$$

$$a_x b_x + a_y b_y = 0 \tag{1.7}$$

where a, b are real functions representing the real and imaginary parts of the eikonal respectively. In [21], Magnanini and Talenti introduced this type of equation by substituting a complex solution with unknown real and imaginary part functions into the eikonal equation (1.1). In their continuation work [22], they establish a Bäcklund transformation between the real part and imaginary part function, and use it to derive a degenerate elliptic second-order partial differential equation for the real part function. They also show that there exists a viscosity solution to the Dirichlet problem of this new equation by using the vanishing viscosity method. In [20], Li, Fomel and Vladimirsky present a numerical approach to the 2D complex eikonal equation. By introducing an intermediate parameter w that decouples (1.6) into two equations

$$b_x^2 + b_y^2 = w^2, \quad a_x^2 + a_y^2 = w^2 + \frac{1}{c^2},$$

they turn the problem into finding the value of w to minimize (1.7) in the linear least-square sense.

Now we start to establish our own model. We assume the solution has the following form

$$\begin{aligned} a(x,y) &= \int_0^y \frac{1}{c(x,s)} ds + x^2 f(x,y), && (1.8) \\ b(x,y) &= x^2 d(y). && (1.9) \end{aligned}$$

By inserting (1.8) and (1.9) into (1.6) and (1.7), and taking certain steps of transformation, we derive a new system of equations

$$x^4(Q - 4x^2c^2d^2)f_x^2 + Qx^4 f_y^2 + 2x^2(Q - 4x^2c^2d^2)(2xf + R)f_x + \frac{2Qx^2 f_y}{c}$$
$$+Q(2xf + R)^2 - 4x^2d^2(Q + c^2(2xf + R)^2) = 0,$$

$$d'(y)(x^3 f_y + \frac{x}{c(x,y)}) + d(y)(2x^2 f_x + 4xf(x,y) - 2\int_0^y \frac{c_x}{c^2(x,s)} ds) = 0$$

where

$$\begin{aligned} R(x,y) &= -\int_0^y \frac{c_x(x,s)}{c^2(x,s)} ds, \\ Q(x,y,f_y) &= (1 + x^2 c(x,y) f_y(x,y))^2. \end{aligned}$$

Noting that $d(y)$ does not depend on the value of x in the second equation for $d(y)$, we freeze x to be a non-zero constant, say x_1, and finally establish a system of equations for $f(x,y)$ and $d(y)$

$$
\begin{aligned}
x^4(Q-4x^2c^2d^2)f_x^2 + Qx^4 f_y^2 + 2x^2(Q-4x^2c^2d^2)(2xf+R)f_x \\
+\frac{2Qx^2 f_y}{c} + Q(2xf+R)^2 - 4x^2d^2(Q+c^2(2xf+R)^2) = 0
\end{aligned} \tag{1.10}
$$

$$
d'(y)(x^3 f_y + \frac{x}{c(x,y)}) + d(y)(2x^2 f_x + 4xf(x,y) - 2\int_0^y \frac{c_x}{c^2(x,s)}ds)\big|_{x=x_1} = 0 \tag{1.11}
$$

In this thesis, we study the initial value problem of (1.10) and (1.11) with the initial conditions $f(x,0)=0$ and $d(0)=\dfrac{1}{2}$ inside the domain $[-1,1]\times[0,2]$. The reason we choose these two initial conditions is that we would like the wave in our model to have a Gaussian profile along the x-axis, which indicates that $a(x,0)=0 \Rightarrow f(x,0)=0$ and $d(0)>0$. Without loss of generality, we let $d(0)=\dfrac{1}{2}$ to endorse the standard Gaussian function. The benefit of this wave having a Gaussian profile at the initial time is that we can use a series of this type of waves with shifted centers to compose a plane wave as shown in [18]. On the other hand, the wave field generated by more complicated sources can often be expressed in terms of a continuous or a discrete spectrum of plane waves, either approximately or exactly (quoted from [7, p.49]). Therefore our model may have potential applications in fields such as seismic imaging and migration.

We would like to give a brief overview of the contents of this thesis. Chapter 2 consists of three sections. In the first section, we give full details of the derivation of (1.10) and (1.11). In the second section, we discuss the solvability of (1.10) with known $d(y)$, and show that (1.10) is equivalent to a system of ordinary differential equations by using the method of characteristics. Based on this system of ordinary differential equations and the ordinary differential equation for $d(y)$, we design a Picard iterative method to show that there exists a local solution to this initial value problem in a domain which stays away from the origin because of (1.10) degenerating on the y-axis. We also give uniqueness of this initial value problem under certain constraints. In the last section, we study the numerical solution of this initial value problem, designing an iterative algorithm to construct two sequences of functions that converge and implementing it in several media. In Chapter 3, we use the theoretical and numerical results from Chapter 2 to design an algorithm to approximate $f(x, y)$ in the domain $[-1, 1] \times [0, 2]$ where we make special efforts to deal with $f(x, y)$ on the y-axis. Next, we derive a partial differential equation for the amplitude $A(x, y)$ and use the Lax-Friedrichs method to solve it with the initial condition $A(x, 0) = 1$. Finally, we implement them to simulate the wave Ae^{a+ib} in various media. In the last chapter, Chapter 4, we establish a numerical scheme for the Helmholtz equation with the Sommerfeld radiation condition, and compare the simulation results with our model's in several media. Next, we perform the degeneracy analysis on (1.10) and (1.11) to derive a system of linear ordinary differential equations for $f(0, y)$ and $d(y)$ and apply the fourth order Runge-Kutta method to solve this system. We use the simulation result of $d(y)$ obtained by this non-iterative method (RK4) to approximate the wave Ae^{a+ib}, and compare the simulation results with our model's in several media. Lastly, we suggest some potential directions of future work.

Chapter 2

Mathematics of Modeling

2.1 Derivation of the Equations

We start with the 2D complex eikonal equation

$$a_x^2 + a_y^2 - b_x^2 - b_y^2 - \frac{1}{c^2(x,y)} = 0, \tag{2.1}$$

$$a_x b_x + a_y b_y = 0. \tag{2.2}$$

Suppose $a(x,y)$ and $b(x,y)$ have the following forms

$$\begin{aligned} a(x,y) &= \int_0^y \frac{1}{c(x,s)} ds + x^2 f(x,y), & (2.3)\\ b(x,y) &= x^2 d(y). & (2.4) \end{aligned}$$

Substituting them into (2.1) and (2.2), we have

$$x^4(f_x^2 + f_y^2) + (4x^3 f - 2x^2 \int_0^y \frac{c_x}{c^2} ds) f_x + \frac{2x^2}{c} f_y + 4x^2 f^2 - 4x(\int_0^y \frac{c_x}{c^2} ds) f$$

$$-x^4 d'^2(y) - 4x^2 d^2(y) + (\int_0^y \frac{c_x}{c^2} ds)^2 = 0, \tag{2.5}$$

$$d'(y)(x^3 f_y + \frac{x}{c(x,y)}) + d(y)(2x^2 f_x + 4x f(x,y) - 2\int_0^y \frac{c_x}{c^2(x,s)} ds) = 0. \tag{2.6}$$

By setting x to be 0 in (2.5), we derive a prerequisite condition on $c(x,y)$

$$\int_0^y \frac{c_x(0,\tau)}{c^2(0,\tau)} d\tau = 0$$

which is equivalent to

$$c_x(0, y) = 0.$$

From (2.6), we derive a formula for $d'(y)$

$$d'(y) = -\frac{2d(y)c(x,y)(x^2 f_x + 2xf - \int_0^y \frac{c_x}{c^2(x,s)}ds)}{x(x^2 c(x,y) f_y + 1)}.$$

Substituting this into (2.5), the equation is transformed into

$$x^4(Q - 4x^2c^2d^2)f_x^2 + Qx^4 f_y^2 + 2x^2(Q - 4x^2c^2d^2)(2xf + R)f_x + \frac{2Qx^2 f_y}{c}$$
$$+Q(2xf + R)^2 - 4x^2d^2(Q + c^2(2xf + R)^2) = 0$$

where

$$\begin{aligned} R(x,y) &= -\int_0^y \frac{c_x(x,s)}{c^2(x,s)}\, ds, \\ Q(x,y,f_y) &= (1 + x^2 c(x,y) f_y(x,y))^2. \end{aligned}$$

Noting that $d(y)$ does not depend on the value of x in (2.6), we may freeze x to be a non-zero value say x_1. So far, we have established a new system of equations for $f(x,y)$ and $d(y)$

$$x^4(Q - 4x^2c^2d^2)f_x^2 + Qx^4 f_y^2 + 2x^2(Q - 4x^2c^2d^2)(2xf + R)f_x$$
$$+\frac{2Qx^2 f_y}{c} + Q(2xf + R)^2 - 4x^2d^2(Q + c^2(2xf + R)^2) = 0 \tag{2.7}$$

$$d'(y)(x^3 f_y + \frac{x}{c(x,y)}) + d(y)(2x^2 f_x + 4xf(x,y) - 2\int_0^y \frac{c_x}{c^2(x,s)}ds)\Big|_{x=x_1} = 0 \tag{2.8}$$

As what we explain on page 9 in Chapter 1, we like the wave in our model to start at the x-axis with a standard Gaussian profile, indicating that

$$a(x,0) = 0 \quad \text{and} \quad d(0) > 0.$$

Therefore we assume the initial conditions for $f(x,y)$ and $d(y)$ are

$$f(x,0) = 0 \quad \text{and} \quad d(0) = \frac{1}{2}. \tag{2.9}$$

2.2 Local Solutions

In this section, we will prove that there exists a local solution to the initial value problem of (2.7) and (2.8) with the initial condition (2.9) in some domain Λ inside $[0,1]\times[0,1]$. Before heading to the local existence theorem, we would like to first discuss (2.7) — the first-order non-linear partial differential equation for $f(x,y)$ — with known $d(y)$.

2.2.1 Nonlinear First-Order PDE for f

Throughout this subsection, we assume $d(y)$ is a known function.

2.2.1.1 Characteristic ODEs

When $d(y)$ is known, (2.7) is a nonlinear first-order partial differential equation for $f(x,y)$. Therefore we can solve it by using the method of characteristics. First, we introduce a curve $(\mathbf{x}(s), \mathbf{y}(s))$ in $\mathbb{R}^2$ where $s \in \overline{\mathbb{R}^+}$ and it starts from some point on the x-axis, say $(x_0, 0)$. The value of f, f_x and f_y

along this curve are denoted by $\mathbf{z}(s)$, $\mathbf{p_1}(s)$ and $\mathbf{p_2}(s)$

$$\mathbf{z}(s) := f(x(s), y(s)),\ \mathbf{p_1}(s) := f_x(x(s), y(s)),\ \mathbf{p_2}(s) := f_y(x(s), y(s)).$$

We write the LHS of (2.7) as a function of x, y, z, p_1 and p_2

$$\begin{aligned} F(x, y, z, p_1, p_2) = {} & x^4(Q - 4x^2c^2d^2){p_1}^2 + Qx^4{p_2}^2 + 2x^2(Q - 4x^2c^2d^2)(2xz + R)p_1 \\ & + \frac{2Qx^2p_2}{c} + Q(2xz + R)^2 - 4x^2d^2(Q + c^2(2xz + R)^2) \end{aligned}$$

where $c = c(x, y)$, $d = d(y)$, $R = R(x, y)$ and $Q = (1 + x^2c(x, y)p_2)^2$.

By the characteristic theory, $\mathbf{x}, \mathbf{y}, \mathbf{z}, \mathbf{p_1}, \mathbf{p_2}$ satisfy the following system of ODEs:

$$\dot{\mathbf{x}}(s) = X(\mathbf{x}(s), \mathbf{y}(s), \mathbf{z}(s), \mathbf{p_1}(s), \mathbf{p_2}(s)) \tag{2.10}$$

$$\dot{\mathbf{y}}(s) = Y(\mathbf{x}(s), \mathbf{y}(s), \mathbf{z}(s), \mathbf{p_1}(s), \mathbf{p_2}(s)) \tag{2.11}$$

$$\dot{\mathbf{z}}(s) = Z(\mathbf{x}(s), \mathbf{y}(s), \mathbf{z}(s), \mathbf{p_1}(s), \mathbf{p_2}(s)) \tag{2.12}$$

$$\dot{\mathbf{p_1}}(s) = U(\mathbf{x}(s), \mathbf{y}(s), \mathbf{z}(s), \mathbf{p_1}(s), \mathbf{p_2}(s)) \tag{2.13}$$

$$\dot{\mathbf{p_2}}(s) = V(\mathbf{x}(s), \mathbf{y}(s), \mathbf{z}(s), \mathbf{p_1}(s), \mathbf{p_2}(s)) \tag{2.14}$$

where

$$
\begin{aligned}
X(x,y,z,p_1,p_2) = \;& 2x^2(Q-4x^2c^2d^2)(2xz+R)+2p_1x^4(Q-4x^2c^2d^2)\\
Y(x,y,z,p_1,p_2) = \;& \frac{2x^2\sqrt{Q}}{c}\Big(1+4p_2x^2c-4d^2x^2c^2+{p_1}^2x^4c^2+2{p_2}^2x^4c^2\\
&+4p_1x^3zc^2+4x^2z^2c^2+2p_1x^2c^2R+4xzc^2R+c^2R^2\Big)\\
Z(x,y,z,p_1,p_2) = \;& \frac{2x^2\sqrt{Q}p_2}{c}\Big(1+4p_2x^2c-4d^2x^2c^2+{p_1}^2x^4c^2+2{p_2}^2x^4c^2\\
&+4p_1x^3zc^2+4x^2z^2c^2+2p_1x^2c^2R+4xzc^2R+c^2R^2\Big)\\
&+2p_1x^2(p_1x^2+2xz+R)(Q-4x^2c^2d^2)\\
U(x,y,z,p_1,p_2) = \;& -4{p_2}^2x^3(Q^2+\frac{\sqrt{Q}J}{c})-\frac{4p_2xQ}{c}-4{p_1}^2x^3(Q-4x^2c^2d^2)\\
&-4p_1x(Q-4x^2c^2d^2)L-4p_1x(L+p_1x^2)(Q-4x^2c^2d^2)\\
&+8xd^2(Q+c^2L^2)+\frac{2p_2x^2Qc_x(x,y)}{c^2}-2{p_2}^3x^5\sqrt{Q}J\\
&-2\Big(p_1x^2(Q-4x^2c^2d^2)+QL\Big)K-2p_2x\sqrt{Q}\,L^2J\\
&-(2{p_1}^2x^5+4p_1x^3L)(-4c^2d^2-4xcd^2c_x(x,y)+p_2\sqrt{Q}J)\\
&+8x^2d^2\Big(c^2LK+cL^2c_x(x,y)+p_2x\sqrt{Q}J\Big)
\end{aligned}
$$

$$
\begin{aligned}
V(x,y,z,p_1,p_2) = \quad & -4p_2x(Q-4x^2d^2c^2)(p_1x^2+L) - 2{p_2}^3x^6\sqrt{Q}c_y(x,y) \\
& -8x^2d^2P(Q+c^2L^2) - \frac{4{p_2}^2x^4\sqrt{Q}c_y(x,y)}{c} \\
& +\frac{2p_2x^2Qc_y(x,y)}{c^2} - 2p_2x^2\sqrt{Q}L^2c_y(x,y) + \frac{2QLc_x(x,y)}{c^2} \\
& -2p_1x^4(p_1x^2+2L)\Big(4c^2d^2P + p_2c_y(x,y) \\
& +cc_y(x,y)({p_2}^2x^2-4d^2)\Big) + \frac{2p_1x^2(Q-4x^2c^2d^2)c_x(x,y)}{c^2} \\
& +4x^2d^2(2p_2x^2\sqrt{Q}c_y(x,y) + 2cL^2c_y(x,y) - 2Lc_x(x,y))
\end{aligned}
$$

with

$$
\begin{aligned}
J &= 2c(x,y) + xc_x(x,y) \\
K &= 2z + \int_0^y \frac{2c_x^2(x,t) - c(x,t)c_{xx}(x,t)}{c^3(x,t)}\,dt \\
L &= 2xz + \int_0^y -\frac{c_x(x,t)}{c(x,t)^2}\,dt \\
P &= \frac{2x^2p_1 + 4xz - 2\displaystyle\int_0^y \frac{c_x(x,t)}{c^2(x,t)}\,dt}{x^3p_2 + \dfrac{x}{c(x,y)}}.
\end{aligned}
$$

2.2.1.2 Initial Conditions

Next, we will find the initial condition of $\mathbf{z}(s), \mathbf{p_1}(s)$ and $\mathbf{p_2}(s)$. We start with the initial condition of $f(x,y)$

$$f(x,0) = 0 \Longrightarrow f_x(x,0) = 0.$$

Thus,

$$\mathbf{z}(0) = \mathbf{p_1}(0) = 0.$$

We set y to be zero in (2.5),

$$x^4 f_y^2(x,0) + \frac{2x^2}{c(x,0)} f_y(x,0) - x^4 d'^2(0) - 4x^2 d^2(0) = 0.$$

From (2.6), it's easy to see $d'(0) = 0$. Thus,

$$x^4 f_y^2(x,0) + \frac{2x^2}{c(x,0)} f_y(x,0) - x^2 = 0.$$

By the quadratic formula,

$$f_y(x,0) = \frac{-1 + \sqrt{1 + c(x,0)^2 x^2}}{c(x,0)x^2}$$

which is also valid at $(0,0)$ by applying a Taylor expansion

$$f_y(0,0) = \frac{1}{2}c(0,0).$$

We assume the characteristic curve $(\mathbf{x}, \mathbf{y})$ starts at $(x_0, 0)$. When $x_0 \neq 0$,

$$\mathbf{p_2}(0) = \frac{-1 + \sqrt{1 + c(x_0,0)^2 x_0^2}}{c(x_0,0)x_0^2} > 0.$$

When $x_0 = 0$, $\mathbf{p_2}(0) = \frac{1}{2}c(0,0)$.

2.2.1.3 Local Invertibility

By the *Local Invertibility* Lemma [16, page 106], if the noncharacteristic condition $F_{p_2} \neq 0$ is valid on some boundary Γ with $\Gamma \subset [0,1] \times \{0\}$, there exists a domain $\Lambda \subset [0,1] \times [0,1]$ with $\partial\Lambda \cap \{y = 0\} = \Gamma$ such that for each $(x,y) \in \Lambda$, there exists a unique pair of x_0 and s such that

$$x = \mathbf{x}(x_0, s) \text{ and } y = \mathbf{y}(x_0, s).$$

The mappings $x, y \mapsto x_0, s$ are C^2. Moreover, the function $f(x,y)$ defined below

$$f(x,y) := \mathbf{z}(x_0(x,y), s(x,y))$$

is a C^2 solution of (2.7) in Λ with the initial condition $f(x,0) = 0$ on Γ. Now let us check where the noncharacteristic condition is satisfied. Recall

$$F_{p_2} = \frac{2x^2\sqrt{Q}}{c}\big(1 + 4p_2x^2c - 4d^2x^2c^2 + {p_1}^2x^4c^2 + 2{p_2}^2x^4c^2 + 4p_1x^3zc^2$$
$$+4x^2z^2c^2 + 2p_1x^2c^2R + 4xzc^2R + c^2R^2\big).$$

Since $\mathbf{x}(0) = x_0$, $\mathbf{y}(0) = 0$, $\mathbf{z}(0) = 0$, $\mathbf{p_1}(0) = 0$ and $\mathbf{p_2}(0) = f_y(x_0, 0)$

$$F_{p_2}(x_0, 0, 0, 0, f_y(x_0, 0)) = \frac{2{x_0}^2\sqrt{Q}}{c}\big(1 + 4p_2(0){x_0}^2c - {x_0}^2c^2 + 2p_2(0)^2{x_0}^4c^2\big).$$

It's clear that $F_{p_2}(x_0, 0, 0, 0, f_y(x_0, 0)) > 0$ in $[\delta, 1]$ with $0 < \delta < 1$. Thus we may assume $\Gamma = [\delta, 1] \times \{0\}$ where δ is a positive number as small as we wish.

From the discussion above, we can make the conclusion that if we have solutions $\mathbf{x}(x_0, s), \mathbf{y}(x_0, s), \mathbf{z}(x_0, s), \mathbf{p_1}(x_0, s), \mathbf{p_2}(x_0, s)$ to (2.10)- (2.14), then there exists a C^2 solution $f(x,y)$ — defined as $\mathbf{z}(x_0(x,y), s(x,y))$ — to (2.7) with the initial condition $f(x,0) = 0$ in a domain Λ. Moreover,

$$f(x,y) = \mathbf{z}(x,y), f_x(x,y) = \mathbf{p_1}(x,y) \text{ and } f_y(x,y) = \mathbf{p_2}(x,y).$$

2.2.2 Local Existence

Noting that $\dot{\mathbf{y}}(0) = F_{p_2}(x_0, 0, 0, 0, f_y(x_0, 0)) > 0$ for any $x_0 \in [\delta, 1]$, we may assume that $\dot{\mathbf{y}}(s) > 0$ in $[0, \theta]$. Hence there exists a one-to-one relation between y and s along this characteristic curve. In light of this, we may consider $\mathbf{x}$, $\mathbf{z}$, $\mathbf{p_1}$ and $\mathbf{p_2}$ as functions of y. Then, $\mathbf{x}(y)$, $\mathbf{z}(y)$, $\mathbf{p_1}(y)$ and $\mathbf{p_2}(y)$ should satisfy

$$
\begin{aligned}
\mathbf{x}_y &= X(\mathbf{x}, y, \mathbf{z}, \mathbf{p_1}, \mathbf{p_2})/Y(\mathbf{x}, y, \mathbf{z}, \mathbf{p_1}, \mathbf{p_2}) &\quad (2.15)\\
\mathbf{z}_y &= Z(\mathbf{x}, y, \mathbf{z}, \mathbf{p_1}, \mathbf{p_2})/Y(\mathbf{x}, y, \mathbf{z}, \mathbf{p_1}, \mathbf{p_2}) &\quad (2.16)\\
\mathbf{p_1}_y &= U(\mathbf{x}, y, \mathbf{z}, \mathbf{p_1}, \mathbf{p_2})/Y(\mathbf{x}, y, \mathbf{z}, \mathbf{p_1}, \mathbf{p_2}) &\quad (2.17)\\
\mathbf{p_2}_y &= V(\mathbf{x}, y, \mathbf{z}, \mathbf{p_1}, \mathbf{p_2})/Y(\mathbf{x}, y, \mathbf{z}, \mathbf{p_1}, \mathbf{p_2}). &\quad (2.18)
\end{aligned}
$$

Moreover, we claim that if $\mathbf{x}(y)$, $\mathbf{z}(y)$, $\mathbf{p_1}(y)$ and $\mathbf{p_2}(y)$ are solutions to (2.15)-(2.18), there exists a function $y(s)$ such that $\mathbf{x}(y(s)), y(s), \mathbf{z}(y(s)), \mathbf{p_1}(y(s))$ and $\mathbf{p_2}(y(s))$ are solutions to (2.10)-(2.14). To show this, we set up a function $s(y)$ as follows

$$s(y) = \int_0^y 1/Y(\mathbf{x}(\tau), \tau, \mathbf{z}(\tau), \mathbf{p_1}(\tau), \mathbf{p_2}(\tau))\, d\tau$$

which leads to

$$s'(y) = 1/Y(\mathbf{x}(y), y, \mathbf{z}(y), \mathbf{p_1}(y), \mathbf{p_2}(y)) \neq 0,$$

otherwise $\mathbf{x}_y, \mathbf{z}_y, \mathbf{p_1}_y, \mathbf{p_2}_y$ would blow out. Thus its inverse function $y(s)$ exists and

$$y'(s) = Y(\mathbf{x}(y(s)), y(s), \mathbf{z}(y(s)), \mathbf{p_1}(y(s)), \mathbf{p_2}(y(s))).$$

Therefore

$$
\begin{aligned}
[\mathbf{x}(y(s))]_s &= \mathbf{x}_y(y(s))y'(s) = X(\mathbf{x}(y(s)), y(s), \mathbf{z}(y(s)), \mathbf{p_1}(y(s)), \mathbf{p_2}(y(s)))\\
[\mathbf{z}(y(s))]_s &= \mathbf{z}_y(y(s))y'(s) = Z(\mathbf{x}(y(s)), y(s), \mathbf{z}(y(s)), \mathbf{p_1}(y(s)), \mathbf{p_2}(y(s)))\\
[\mathbf{p_1}(y(s))]_s &= \mathbf{p_1}_y(y(s))y'(s) = U(\mathbf{x}(y(s)), y(s), \mathbf{z}(y(s)), \mathbf{p_1}(y(s)), \mathbf{p_2}(y(s)))\\
[\mathbf{p_2}(y(s))]_s &= \mathbf{p_2}_y(y(s))y'(s) = V(\mathbf{x}(y(s)), y(s), \mathbf{z}(y(s)), \mathbf{p_1}(y(s)), \mathbf{p_2}(y(s)))
\end{aligned}
$$

which implies that $\mathbf{x}(s)$, $\mathbf{z}(s)$, $\mathbf{p_1}(s)$, $\mathbf{p_2}(s)$ — defined as $\mathbf{x}(y(s))$, $\mathbf{z}(y(s))$, $\mathbf{p_1}(y(s))$, $\mathbf{p_2}(y(s))$ — and $y(s)$ are solutions of (2.10)- (2.14). In light of the equivalence between these two systems of ODEs (2.10)- (2.14) and (2.15)- (2.18), we can have the local existence result by finding solutions to (2.15)- (2.18).

Theorem 2.2.1 (Local Existence Theorem)**.** *There exists a domain* Λ

$$\Lambda \subset [0,1] \times [0,1] \quad \textit{and} \quad \partial\Lambda \cap \{y=0\} = \Gamma$$

such that over the domain Λ*, there exists a solution —* $f(x,y)$ *and* $d(y)$ *— to the initial value problem of*

$$\begin{aligned} x^4(Q-4x^2c^2d^2)f_x^2 + Qx^4f_y^2 + 2x^2(Q-4x^2c^2d^2)(2xf+R)f_x & \\ + \frac{2Qx^2f_y}{c} + Q(2xf+R)^2 - 4x^2d^2(Q+c^2(2xf+R)^2) &= 0 \\ d'(y)(x^3f_y + \frac{x}{c(x,y)}) + d(y)(2x^2f_x + 4xf(x,y) - 2\int_0^y \frac{c_x}{c^2(x,s)}ds)\big|_{x=x_1} &= 0 \end{aligned}$$

with the initial conditions

$$f(x,0)=0, \;\; d(0) = \frac{1}{2} \; .$$

Proof. We will establish this theorem by designing *Picard's* iterative method to construct iterative sequences of $x_n(y)$, $z_n(y)$, $p_{1n}(y)$, $p_{2n}(y)$ and $d_n(y)$ such that the curve $(x_n(y), y)$ has an initial point of $(x_0, 0)$, z_n, p_{1n}, p_{2n} are the approximations of f, f_x, f_y along the curve $(x_n(y), y)$, and $d_n(y)$ is the approximation of $d(y)$. Before beginning the proof, we first introduce some notations

$$\alpha = (x, z, p_1, p_2), \alpha_n = (x_n, z_n, p_{1n}, p_{2n}),$$

$$\begin{aligned}
&F_1 = X(\alpha, d, y)/Y(\alpha, d, y), F_2 = Z(\alpha, d, y)/Y(\alpha, d, y),\\
&F_3 = U(\alpha, d, y)/Y(\alpha, d, y), F_4 = V(\alpha, d, y)/Y(\alpha, d, y),\\
&F_1^n = F_1(\alpha_n, d_n, y), F_2^n = F_2(\alpha_n, d_n, y),\\
&F_3^n = F_3(\alpha_n, d_n, y), F_4^n = F_4(\alpha_n, d_n, y).
\end{aligned}$$

The iterative sequences of $x_n, y_n, z_n, p_{1n}, p_{2n}$ and d_n are constructed as follows

1. Assume $d_0 = \dfrac{1}{2}$, $\alpha_0 = (x_0, 0, 0, \eta(x_0))$ where $\eta(x_0) = \dfrac{-1 + \sqrt{1 + c(x_0, 0)^2 x_0^2}}{c(x_0, 0) x_0^2}$.

2. α_{n+1} and d_{n+1} are given by

$$\alpha_{n+1}(j) = \mu(j) + \textstyle\int_0^y F_j^n d\tau, \quad j = 1 \text{ to } 4$$

$$d_{n+1} = \frac{1}{2} e^{-\int_0^y P\left(z_n(x_1, \tau), p_{1n}(x_1, \tau), p_{2n}(x_1, \tau), \tau\right) d\tau}$$

where $\mu = \alpha_0$ and

$$P(z, p_1, p_2, y) = \frac{2{x_1}^2 p_1 + 4 x_1 z - 2 \displaystyle\int_0^y \frac{c_{x_1}(x_1, t)}{c^2(x_1, t)}\, dt}{{x_1}^3 p_2 + \dfrac{x_1}{c(x_1, y)}}.$$

If x_n, z_n, p_{1n}, p_{2n} and d_n are uniformly convergent to some functions — namely $\mathbf{x}, \mathbf{z}, \mathbf{p_1}, \mathbf{p_2}$ and $\mathbf{d}$, then

$$\mathbf{d} = \frac{1}{2} e^{-\int_0^y P\left(\mathbf{z}(x_1, \tau), \mathbf{p_1}(x_1, \tau), \mathbf{p_2}(x_1, \tau), \tau\right) d\tau} \tag{2.19}$$

$$\mathbf{x}_y = X(\mathbf{x}, y, \mathbf{z}, \mathbf{p_1}, \mathbf{p_2})/Y(\mathbf{x}, y, \mathbf{z}, \mathbf{p_1}, \mathbf{p_2}) \tag{2.20}$$

$$\mathbf{z}_y = Z(\mathbf{x}, y, \mathbf{z}, \mathbf{p_1}, \mathbf{p_2})/Y(\mathbf{x}, y, \mathbf{z}, \mathbf{p_1}, \mathbf{p_2}) \tag{2.21}$$

$$\mathbf{p_1}_y = U(\mathbf{x}, y, \mathbf{z}, \mathbf{p_1}, \mathbf{p_2})/Y(\mathbf{x}, y, \mathbf{z}, \mathbf{p_1}, \mathbf{p_2}) \tag{2.22}$$

$$\mathbf{p_2}_y = V(\mathbf{x}, y, \mathbf{z}, \mathbf{p_1}, \mathbf{p_2})/Y(\mathbf{x}, y, \mathbf{z}, \mathbf{p_1}, \mathbf{p_2})\,. \tag{2.23}$$

(2.19) gives an explicit formula for $\mathbf{d}(y)$, hence we can consider $\mathbf{d}$ term in every characteristic ODE of (2.20)-(2.23) as a function of y. Simultaneously $\mathbf{x}, \mathbf{z}, \mathbf{p_1}, \mathbf{p_2}$ satisfy (2.20)-(2.23). Therefore there exists a C^2 function $f(x,y)$ in some domain Λ such that $f(x,y)$ is a solution to (2.7) with known $\mathbf{d}(y)$ and

$$f(x,y) = \mathbf{z}(x,y), f_x(x,y) = \mathbf{p_1}(x,y), f_y(x,y) = \mathbf{p_2}(x,y).$$

Simultaneously,

$$\mathbf{d}'(y) = -P(f(x_1,y), f_x(x_1,y), f_y(x_1,y), y)\mathbf{d}(y)$$

which is equivalent to (2.8).

The discussion above indicates that as long as we can prove the hypothesis that $x_n, y_n, z_n, p_{1n}, p_{2n}$ and d_n are uniformly convergent, the proof of local existence will be complete. In fact, this hypothesis can be proved with the following steps.

Step 1. Set up a priori conditions.

We set up the following two a priori conditions

1. For all $n \geq 1$,

$$\boxed{||d_n|| + ||\alpha_n|| < ||d_0|| + ||\alpha_0|| + 1} \tag{2.24}$$

   where $||\alpha_n|| = \sum_{j=1}^{4} ||\alpha_n(j)||$.

2. There exists a constant $\gamma > 0$ such that for all $n \geq 0$

$$\boxed{x_{nx_0} > \frac{1}{\gamma}} \tag{2.25}$$

where $||\cdot||$ is the maximum norm of the function.

Let

$$\begin{aligned}
\Psi &= [-||d_0|| - ||\alpha_0|| - 1, ||d_0|| + ||\alpha_0|| + 1]^5 \subset \mathbb{R}^5 \\
||F_j|| &= \max_{(\alpha,d)\in\Psi, y\in[0,1]} |F_j(\alpha, d, y)| \\
||F|| &= \sum_{j=1}^{4} ||F_j|| \\
||\nabla F_j|| &= \max_{(\alpha,d)\in\Psi, y\in[0,1]} |\nabla F_j(\alpha, d, y)| \\
||\nabla F|| &= \sum_{j=1}^{4} ||\nabla F_j|| \\
||P|| &= \max_{(\alpha,d)\in\Psi, y\in[0,1]} |P(z, p_1, p_2, y)| \\
||\nabla P|| &= \max_{(\alpha,d)\in\Psi, y\in[0,1]} |\nabla P(z, p_1, p_2, y)|
\end{aligned}$$

where $|\nabla(\cdot)|$ is the sum of the absolute value of all its first derivatives.

Step 2. Find the estimations.

With all the bounds defined in **Step 1**, our ultimate goal in this step is to have the estimation of the following functions

(a) $|\alpha_{nx_0}|$

(b) $|\alpha_n - \alpha_0| + |d_n - d_0|$

(c) $|x_{nx_0} - x_{0x_0}|$

where $|\alpha_{nx_0}| = \sum_{j=1}^{4} |\alpha_n(j)_{x_0}|$ and $|\alpha_m - \alpha_n| = \sum_{j=1}^{4} |\alpha_m(j) - \alpha_n(j)|$.

Start with (a). Supposing α and d are solutions to (2.19)-(2.23),

$$[\alpha_{x_0}(j)]_y = \sum_{k=1}^{4} \partial_k F_j(\alpha, d, y)\alpha_{x_0}(k)$$

due to $d(y)_{x_0} = 0$. Then,

$$|\alpha_{x_0}(j)|_y \leq ||\nabla F_j|| \sum_{k=1}^{4} |\alpha_{x_0}(k)| \leq ||\nabla F_j||\,|\alpha_{x_0}|.$$

Combining all the inequalities with j from 1 to 4,

$$|\alpha_{x_0}|_y \leq ||\nabla F||\,|\alpha_{x_0}|.$$

By *Gronwall's Inequality*

$$|\alpha_{x_0}| \leq e^{||\nabla F||y}|\alpha_{x_0}(0)| \leq e^{||\nabla F||y}(1 + ||\eta_{x_0}||).$$

Next, we will prove that for all $n \geq 0$

$$\boxed{|\alpha_{nx_0}| \leq e^{||\nabla F||y}(1 + ||\eta_{x_0}||)}. \tag{2.26}$$

When $n = 0$,

$$|\alpha_{0x_0}| \leq (1 + ||\eta_{x_0}||)$$

thus (2.26) holds.

Assume (2.26) holds for n and recall the formula for $\alpha_{n+1_{x_0}}(j)$

$$\alpha_{n+1_{x_0}}(j) = \mu(j)_{x_0} + \int_0^y \sum_{k=1}^4 \partial_k F_j(\alpha_n, d_n, \tau)\alpha_{nx_0}(k)\, d\tau.$$

Then,

$$\begin{aligned} |\alpha_{n+1_{x_0}}| &\leq (1 + ||\eta_{x_0}||) + ||\nabla F||(1 + ||\eta_{x_0}||) \textstyle\int_0^y e^{||\nabla F||\tau}\, d\tau \\ &\leq (1 + ||\eta_{x_0}||) + (1 + ||\eta_{x_0}||)(e^{||\nabla F||y} - 1) \\ &\leq (1 + ||\eta_{x_0}||)e^{||\nabla F||y} \end{aligned}$$

thus (2.26) holds for $n+1$. By mathematical induction, (2.26) holds for all $n \geq 0$.

Next, we will estimate (b). Start with $|\alpha_{n+1} - \alpha_n|$ and $|d_{n+1} - d_n|$

$$\begin{aligned} |\alpha_{n+1} - \alpha_n| \leq & \textstyle\sum_{j=1}^4 \int_0^y |F_j^n - F_j^{n-1}|\, d\tau \\ \leq & \textstyle\sum_{j=1}^4 ||\nabla F_j|| \int_0^y |\alpha_n - \alpha_{n-1}| + |d_n - d_{n-1}|\, d\tau \\ \leq & ||\nabla F|| \textstyle\int_0^y |\alpha_n - \alpha_{n-1}| + |d_n - d_{n-1}|\, d\tau \\ |d_{n+1} - d_n| = & \frac{1}{2}|e^{-\int_0^y P(\beta_n, y)\, d\tau} - e^{-\int_0^y P(\beta_{n-1}, y)\, d\tau}| \\ \leq & \frac{1}{2}e^{||P||} \textstyle\int_0^y |P(\beta_n, y) - P(\beta_{n-1}, y)|\, d\tau \\ \leq & \frac{1}{2}e^{||P||}||\nabla P|| \int_0^y |\beta_n - \beta_{n-1}|\, d\tau \end{aligned}$$

where $\beta_n = \big(z_n(x_0^n(x_1,y),y), p_{1n}(x_0^n(x_1,y),y), p_{2n}(x_0^n(x_1,y),y)\big)$ and

$$|\beta_n - \beta_{n-1}| = \sum_{j=1}^{3} |\beta_n(j) - \beta_{n-1}(j)|.$$

We first calculate $|\beta_n(1) - \beta_{n-1}(1)|$

$$\begin{aligned}
& |z_n(x_0^n(x_1,y),y) - z_{n-1}(x_0^{n-1}(x_1,y),y)| \\
\leq \;& |z_n(x_0^n(x_1,y),y) - z_n(x_0^{n-1}(x_1,y),y)| \\
& \qquad\qquad + |z_n(x_0^{n-1}(x_1,y),y) - z_{n-1}(x_0^{n-1}(x_1,y),y)| \\
\leq \;& ||z_{nx_0}|||x_0^n(x_1,y) - x_0^{n-1}(x_1,y)| + |z_n - z_{n-1}|\big|_{x_0^{n-1}(x_1,y)}.
\end{aligned}$$

Noting

$$x_n(x_0^n(x_1,y),y) = x_{n-1}(x_0^{n-1}(x_1,y),y) = x_1$$

$$\Downarrow$$

$$\begin{aligned}
& |x_{n-1}(x_0^{n-1}(x_1,y),y) - x_{n-1}(x_0^n(x_1,y),y)| \\
= \;& |x_n(x_0^n(x_1,y),y) - x_{n-1}(x_0^n(x_1,y),y)| \\
\leq \;& |x_n - x_{n-1}|\big|_{x_0^n(x_1,y)}
\end{aligned}$$

then

$$\begin{aligned}
& |x_0^n(x_1,y) - x_0^{n-1}(x_1,y)| \\
= \;& |x_0^{n-1}(x_{n-1}(x_0^n(x_1,y),y),y) - x_0^{n-1}(x_{n-1}(x_0^{n-1}(x_1,y),y),y)| \\
\leq \;& ||x_{0x}^{n-1}||\,|x_n - x_{n-1}|\big|_{x_0^n(x_1,y)} \\
\leq \;& \gamma |x_n - x_{n-1}|\big|_{x_0^n(x_1,y)}
\end{aligned}$$

due to $x_{0x}^n = \dfrac{1}{x_{nx_0}}$.

Therefore,

$$
\begin{aligned}
& |z_n(x_0^n(x_1,y),y) - z_{n-1}(x_0^{n-1}(x_1,y),y)| \\
\leq \; & \gamma ||z_{nx_0}|| |x_n - x_{n-1}| \big|_{x_0^n(x_1,y)} + |z_n - z_{n-1}| \big|_{x_0^{n-1}(x_1,y)} .
\end{aligned}
$$

Similarly,

$$
\begin{aligned}
& |p_{1n}(x_0^n(x_1,y),y) - p_{1n-1}(x_0^{n-1}(x_1,y),y)| \\
\leq \; & \gamma ||p_{1nx_0}|| |x_n - x_{n-1}| \big|_{x_0^n(x_1,y)} + |p_{1n} - p_{1n-1}| \big|_{x_0^{n-1}(x_1,y)} \\
& |p_{2n}(x_0^n(x_1,y),y) - p_{2n-2}(x_0^{n-2}(x_1,y),y)| \\
\leq \; & \gamma ||p_{2nx_0}|| |x_n - x_{n-1}| \big|_{x_0^n(x_1,y)} + |p_{2n} - p_{2n-1}| \big|_{x_0^{n-1}(x_1,y)} .
\end{aligned}
$$

In summary,

$$
\begin{aligned}
& |d_{n+1} - d_n| \\
\leq \; & \frac{1}{2} e^{||P||} ||\nabla P|| (\gamma ||\alpha_{nx_0}|| + 1) \int_0^y |x_n - x_{n-1}| \big|_{x_0^n(x_1,\tau)} \\
& + |\alpha_n - \alpha_{n-1}| \big|_{x_0^{n-1}(x_1,\tau)} \, d\tau \\
\leq \; & \frac{1}{2} e^{||P||} ||\nabla P|| \big(\gamma (1 + ||\eta_{x_0}||) e^{||\nabla F||} + 1\big) \int_0^y |\alpha_n - \alpha_{n-1}| \big|_{x_0^n(x_1,\tau)} \\
& + |\alpha_n - \alpha_{n-1}| \big|_{x_0^{n-1}(x_1,\tau)} \, d\tau
\end{aligned}
$$

due to (2.26).

Therefore

$$
\begin{aligned}
& |\alpha_{n+1} - \alpha_n| + |d_{n+1} - d_n| \\
\leq \quad & E\Big(\textstyle\int_0^y |\alpha_n - \alpha_{n-1}|\big|_{x_0} + |d_n - d_{n-1}|\, d\tau \\
& + \textstyle\int_0^y |\alpha_n - \alpha_{n-1}|\big|_{x_0^n(x_1,\tau)} + |d_n - d_{n-1}|\, d\tau \\
& + \textstyle\int_0^y |\alpha_n - \alpha_{n-1}|\big|_{x_0^{n-1}(x_1,\tau)} + |d_n - d_{n-1}|\, d\tau \Big)
\end{aligned}
$$

where $E = ||\nabla F|| + \dfrac{1}{2} e^{||P||} ||\nabla P|| \big(\gamma(1 + ||\eta_{x_0}||) e^{||\nabla F||} + 1 \big)$.

Now we start to estimate $|\alpha_1 - \alpha_0| + |d_1 - d_0|$ and first recall the formula for α_1

$$\alpha_1(j) = \alpha_0(j) + \int_0^y F_j(\alpha_0, d_0, \tau)\, d\tau, \quad j = 1 \text{ to } 4.$$

Then,

$$|\alpha_1 - \alpha_0| \leq ||F|| y$$

$$|d_1 - d_0| = |d_1(y) - d_1(0)| \leq ||d_1'|| y$$

thus

$$|\alpha_1 - \alpha_0| + |d_1 - d_0| \leq (||d_1'|| + ||F||) y.$$

Next we will show that for all $n \geq 1$

$$|\alpha_{n+1} - \alpha_n| + |d_{n+1} - d_n| \leq (||d_1'|| + ||F||)(3E)^n \frac{y^{n+1}}{(n+1)!}\,. \tag{2.27}$$

Assuming (2.27) holds for $n-1$

$$
\begin{aligned}
& |\alpha_{n+1}-\alpha_n|+|d_{n+1}-d_n| \\
\leq\ & E\Big(\textstyle\int_0^y |\alpha_n-\alpha_{n-1}|\big|_{x_0}+|d_n-d_{n-1}|\,d\tau \\
& + \textstyle\int_0^y |\alpha_n-\alpha_{n-1}|\big|_{x_0^n(x_1,\tau)}+|d_n-d_{n-1}|\,d\tau \\
& + \textstyle\int_0^y |\alpha_n-\alpha_{n-1}|\big|_{x_0^{n-1}(x_1,\tau)}+|d_n-d_{n-1}|\,d\tau\Big) \\
\leq\ & 3E\textstyle\int_0^y(||d_1'||+||F||)(3E)^{n-1}\dfrac{\tau^n}{n!}\,d\tau \\
\leq\ & (||d_1'||+||F||)(3E)^n\dfrac{y^{n+1}}{(n+1)!}
\end{aligned}
$$

thus (2.27) holds for all $n\geq 0$ by induction.

Moreover,

$$|\alpha_n-\alpha_0|+|d_n-d_0|\leq\sum_{j=1}^{n}|\alpha_j-\alpha_{j-1}|+|d_j-d_{j-1}|\leq\sum_{j=1}^{n}(||d_1'||+||F||)(3E)^{j-1}\frac{y^j}{j!}$$

hence

$$\boxed{|\alpha_n-\alpha_0|+|d_n-d_0|\leq(||d_1'||+||F||)e^{3E}y}.$$

Now we begin estimating (c). Recall

$$
\begin{aligned}
\alpha_{n+1}(j)_{x_0} &= \mu(j)_{x_0}+\textstyle\int_0^y\sum_{k=1}^4\partial_kF_j(\alpha_n,d_n,\tau)\alpha_{n x_0}(k)\,d\tau \\
\alpha_n(j)_{x_0} &= \mu(j)_{x_0}+\textstyle\int_0^y\sum_{k=1}^4\partial_kF_j(\alpha_{n-1},d_{n-1},\tau)\alpha_{n-1 x_0}(k)\,d\tau.
\end{aligned}
$$

Then,

$$
\begin{aligned}
& |\alpha_{n+1}(j)_{x_0} - \alpha_n(j)_{x_0}| \\
\leq\ & \textstyle\sum_{k=1}^4 \int_0^y |\partial_k F_j(\alpha_n, d_n, \tau)\alpha_{nx_0}(k) - \partial_k F_j(\alpha_{n-1}, d_{n-1}, \tau)\alpha_{n-1_{x_0}}(k)|\, d\tau \\
\leq\ & \textstyle\sum_{k=1}^4 \int_0^y |\partial_k F_j(\alpha_n, d_n, \tau)\alpha_{nx_0}(k) - \partial_k F_j(\alpha_{n-1}, d_{n-1}, \tau)\alpha_{nx_0}(k)| \\
& +|\partial_k F_j(\alpha_{n-1}, d_{n-1}, \tau)\alpha_{nx_0}(k) - \partial_k F_j(\alpha_{n-1}, d_{n-1}, \tau)\alpha_{n-1_{x_0}}(k)|\, d\tau \\
\leq\ & \textstyle\sum_{k=1}^4 \int_0^y |\partial_k F_j(\alpha_n, d_n, \tau) - \partial_k F_j(\alpha_{n-1}, d_{n-1}, \tau)|\, |\alpha_{nx_0}(k)|\, d\tau \\
& + \textstyle\sum_{k=1}^4 \int_0^y |\partial_k F_j(\alpha_{n-1}, d_{n-1}, \tau)|\, |\alpha_{nx_0}(k) - \alpha_{n-1_{x_0}}(k)|\, d\tau \\
\leq\ & \textstyle\sum_{k=1}^4 \int_0^y (\sum_{l=1}^5 |\partial_l \partial_k F_j|)(|\alpha_n - \alpha_{n-1}| + |d_n - d_{n-1}|)|\alpha_{nx_0}(k)|\, d\tau \\
& +||\nabla F_j|| \textstyle\int_0^y\, |\alpha_{nx_0} - \alpha_{n-1_{x_0}}|\, d\tau \\
\leq\ & ||\alpha_{nx_0}||\, ||\partial^2 F_j|| \textstyle\int_0^y |\alpha_n - \alpha_{n-1}| + |d_n - d_{n-1}|\, d\tau \\
& +||\nabla F_j|| \textstyle\int_0^y\, |\alpha_{nx_0} - \alpha_{n-1_{x_0}}|\, d\tau
\end{aligned}
$$

where k and l denote the kth and lth component of the function and $||\partial^2 F_j|| = \sum_{k=1}^{6}\sum_{l=1}^{6} \max_{(\alpha,d)\in\Psi, y\in[0,1]} |\partial^2_{k,l} F_j|$.

Adding up all the inequalities with j from 1 to 4,

$$
\begin{aligned}
& |\alpha_{n+1_{x_0}} - \alpha_{nx_0}| \\
\leq\ & e^{||\nabla F||}(1 + ||\eta_{x_0}||)||\partial^2 F|| \textstyle\int_0^y |\alpha_n - \alpha_{n-1}| + |d_n - d_{n-1}|\, d\tau \\
& +||\nabla F|| \textstyle\int_0^y |\alpha_{nx_0} - \alpha_{n-1_{x_0}}|\, d\tau \\
\leq\ & M(3E)^{n-1}\frac{y^{n+1}}{(n+1)!} + 3E \textstyle\int_0^y |\alpha_{nx_0} - \alpha_{n-1_{x_0}}|\, d\tau
\end{aligned}
$$

where $||\partial^2 F|| = \sum_{j=1}^{4} ||\partial^2 F_j||$ and $M = (||d_1'|| + ||F||)(1 + ||\eta_{x_0}||)||\partial^2 F||e^{||\nabla F||}$.

When $n = 1$,

$$\alpha_{1x_0}(j) = \alpha_{0x_0}(j) + \int_0^y \sum_{k=1}^{4} \partial_k F_j(\alpha_0, d_0, \tau)\alpha_{0x_0}(k)\, d\tau$$

therefore

$$|\alpha_1 - \alpha_0| \le ||\nabla F|| \cdot ||\alpha_{0x_0}||y \le ||\nabla F||(1 + ||\eta_{x_0}||)y\,.$$

Next, we will prove that for all $n \ge 1$

$$|\alpha_{nx_0} - \alpha_{n-1x_0}| \le (n-1)M(3E)^{n-2}\frac{y^n}{n!} + ||\nabla F||(1+||\eta_{x_0}||)(3E)^{n-1}\frac{y^n}{n!}\,. \quad (2.28)$$

Clearly, (2.28) holds for $n = 0$. Assuming (2.28) holds for n

$$\begin{aligned}
& |\alpha_{n+1x_0} - \alpha_{nx_0}| \\
\le\ & M(3E)^{n-1}\frac{y^{n+1}}{(n+1)!} + 3E\textstyle\int_0^y |\alpha_{nx_0} - \alpha_{n-1x_0}|\, d\tau \\
\le\ & M(3E)^{n-1}\frac{y^{n+1}}{(n+1)!} + (n-1)M(3E)^{n-1}\frac{y^{n+1}}{(n+1)!} \\
& \qquad + ||\nabla F||(1 + ||\eta_{x_0}||)(3E)^n\frac{y^{n+1}}{(n+1)!} \\
\le\ & n\, M(3E)^{n-1}\frac{y^{n+1}}{(n+1)!} + +||\nabla F||(1 + ||\eta_{x_0}||)(3E)^n\frac{y^{n+1}}{(n+1)!}
\end{aligned}$$

thus (2.28) holds for $n+1$. By induction, (2.28) holds for all $n \ge 1$.

Therefore

$$\begin{aligned}|\alpha_{nx_0} - \alpha_{0x_0}| &\leq \textstyle\sum_{j=1}^{n} |\alpha_{j_{x_0}} - \alpha_{j-1_{x_0}}| \\ &\leq \textstyle\sum_{j=1}^{n} (j-1)M(3E)^{j-2}\dfrac{y^j}{j!} + ||\nabla F||(1+||\eta_{x_0}||)(3E)^{j-1}\dfrac{y^j}{j!} \\ &\leq (M/3E)e^{3Ey}y + ||\nabla F||(1+||\eta_{x_0}||)e^{3Ey}y \\ &\leq [(M/3E)e^{3E} + ||\nabla F||(1+||\eta_{x_0}||)e^{3E}]\, y\,.\end{aligned}$$

Simultaneously,

$$\boxed{|x_{nx_0} - x_{0x_0}| \leq [(M/3E)e^{3E} + ||\nabla F||(1+||\eta_{x_0}||)e^{3E}]\, y}\,.$$

Step 3. Find the domain.

In this step, we are going to find a domain Θ

$$\Theta := \{(x_0, y)|\, x_0 \in [\delta, 1],\, y \in [0, \theta] \text{ with } \delta > 0, \theta < 1\}$$

such that a priori conditions (2.24) and (2.25) hold in Θ.

Let $\theta = ((||d_1'|| + ||F||)e^{3E} + 1)^{-1}$

$$|\alpha_n - \alpha_0| + |d_n - d_0| \leq (||d_1'|| + ||F||)e^{3E}y \leq (||d_1'|| + ||F||)e^{3E}\theta < 1$$

which implies (2.24)

$$|d_n| + |\alpha_n| \leq |d_n - d_0| + |d_0| + |\alpha_n - \alpha_0| + |\alpha_0| < |d_0| + |\alpha_0| + 1.$$

Since

$$x_{0x_0} = 1 + \int_0^y \sum_{k=1}^4 \partial_k F_1(\alpha_0, d_0, \tau)\alpha_{0x_0}(k)\, d\tau,$$

there exists $\lambda > 0$ such that $x_{0x_0} > \dfrac{2}{\gamma}$ in $[\delta, 1] \times [0, \lambda]$. Then

$$\begin{aligned} x_{nx_0} = &\ \ x_{nx_0} - x_{0x_0} + x_{0x_0} \\ \geq &\ \ x_{0x_0} - |x_{nx_0} - x_{0x_0}| \\ > &\ \ \frac{2}{\gamma} - [(M/3E)e^{3E} + ||\nabla F||(1 + ||\eta_{x_0}||)e^{3E}]\theta. \end{aligned}$$

Let $\theta = \min\big(\theta, \lambda, \dfrac{1}{\gamma}[(M/3E)e^{3E} + ||\nabla F||(1 + ||\eta_{x_0}||)e^{3E}]^{-1}\big)$

$$x_{nx_0} > \frac{1}{\gamma}.$$

Hence (2.25) holds.

Step 4. Prove the uniform convergence.

In this final step, we will complete our proof by proving the hypothesis that $x_n, y_n, z_n, p_{1n}, p_{2n}$ and d_n are uniformly convergent. First recall (2.27)

$$|\alpha_{n+1} - \alpha_n| + |d_{n+1} - d_n| \leq (||d_1'|| + ||F||)(3E)^n \frac{y^{n+1}}{(n+1)!}.$$

For any $m > n$,

$$
\begin{aligned}
& |\alpha_m - \alpha_n| + |d_m - d_n| \\
\leq & \sum_{k=n+1}^{m} |\alpha_k - \alpha_{k-1}| + |d_k - d_{k-1}| \\
\leq & \sum_{k=n+1}^{m} \frac{||d_1'|| + ||F||}{3E} \frac{(3Ey)^k}{k!}.
\end{aligned}
$$

Since the series $\sum_{k=0}^{\infty} \frac{||d_1'|| + ||F||}{3E} \frac{(3Ey)^k}{k!}$ is uniformly convergent in $[0, \theta]$, the sequences of functions x_n, y_n, z_n, p_{1n}, p_{2n} and d_n are uniformly convergent. $\square$

2.2.3 Uniqueness

We have already established local existence and now we will prove uniqueness under certain constraints.

Theorem 2.2.2 (Uniqueness Theorem). *Suppose there are two solutions — $\tilde{f}, \tilde{d}$ and $\hat{f}, \hat{d}$ — to the initial value problem of*

$$
\begin{aligned}
x^4(Q - 4x^2c^2d^2)f_x^2 + Qx^4 f_y^2 + 2x^2(Q - 4x^2c^2d^2)(2xf + R)f_x & \\
+\frac{2Qx^2 f_y}{c} + Q(2xf + R)^2 - 4x^2d^2(Q + c^2(2xf + R)^2) &= 0 \\
d'(y)(x^3 f_y + \frac{x}{c(x,y)}) + d(y)(2x^2 f_x + 4xf(x,y) - 2\int_0^y \frac{c_x}{c^2(x,s)} ds)\big|_{x=x_1} &= 0
\end{aligned}
$$

with the initial conditions

$$
f(x, 0) = 0, \;\; d(0) = \frac{1}{2}
$$

in the domain Λ defined as

$$
\Lambda \subset [0, 1] \times [0, 1] \;\; and \;\; \partial\Lambda \cap \{y = 0\} = \Gamma.
$$

If both of the solutions satisfy

$$Y(x, y, f(x, y), f_x(x, y), f_y(x, y), d(y)) \neq 0 \quad in\ \Lambda,$$

then

$$\tilde{f} = \hat{f}, \quad \tilde{d} = \hat{d} \quad in\ \Lambda.$$

Proof. Due to

$$Y(x, y, \tilde{f}(x, y), \tilde{f}_x(x, y), \tilde{f}_y(x, y), \tilde{d}(y)) \neq 0$$

$$Y(x, y, \hat{f}(x, y), \hat{f}_x(x, y), \hat{f}_y(x, y), \hat{d}(y)) \neq 0,$$

there exist two sets of characteristic functions of y — $\tilde{\alpha} = (\tilde{x}, \tilde{z}, \tilde{p}_1, \tilde{p}_2)$ and $\hat{\alpha} = \hat{x}, \hat{z}, \hat{p}_1, \hat{p}_2$ — such that they are solutions to (2.15)-(2.18)

$$\tilde{\alpha}(j) = \mu(j) + \textstyle\int_0^y F_j(\tilde{\alpha}, \tilde{d}, y)\, d\tau, \quad j = 1 \text{ to } 4$$

$$\hat{\alpha}(j) = \mu(j) + \textstyle\int_0^y F_j(\hat{\alpha}, \hat{d}, y)\, d\tau, \quad j = 1 \text{ to } 4$$

where $\mu(j)$ is the initial condition.

Since

$$\tilde{x}_{x_0}(0) = \hat{x}_{x_0}(0) = 1,$$

there exists $\theta > 0$ such that for any $(x, y) \in \Lambda \cap [0, 1] \times [0, \theta]$, there exist $\tilde{x}_0(x, y)$ and $\hat{x}_0(x, y)$ such that

$$\tilde{z}(\tilde{x}_0(x, y), y) = \tilde{f}(x, y), \;\; \tilde{p}_1(\tilde{x}_0(x, y), y) = \tilde{f}_x(x, y), \;\; \tilde{p}_2(\tilde{x}_0(x, y), y) = \tilde{f}_y(x, y),$$

$$\hat{z}(\hat{x}_0(x, y), y) = \hat{f}(x, y), \;\; \hat{p}_1(\hat{x}_0(x, y), y) = \hat{f}_x(x, y), \;\; \hat{p}_2(\hat{x}_0(x, y), y) = \hat{f}_y(x, y).$$

Let

$$\begin{aligned} m &= 1 + ||\tilde{f}|| + ||\tilde{f}_x|| + ||\tilde{f}_y|| + 1 + ||\hat{f}|| + ||\hat{f}_x|| + ||\hat{f}_y|| + ||\tilde{d}|| + ||\hat{d}|| \\ \Psi &= [-m, m] \times [-m, m] \times [-m, m] \times [-m, m] \times [-m, m] \subset \mathbb{R}^5 \end{aligned}$$

where $|| \cdot || = \max\limits_{(x,y)\in\, \Lambda\cap[0,1]\times[0,\theta]} | \cdot |$.

Define the following bounds

$$\begin{aligned} ||F_j|| &= \max_{(\alpha,d)\in\Psi, y\in[0,1]} |F_j(\alpha, d, y)| \\ ||F|| &= \sum_{j=1}^{4} ||F_j|| \\ ||\nabla F_j|| &= \max_{(\alpha,d)\in\Psi, y\in[0,1]} |\nabla F_j(\alpha, d, y)| \\ ||\nabla F|| &= \sum_{j=1}^{4} ||\nabla F_j|| \\ ||P|| &= \max_{(\alpha,d)\in\Psi, y\in[0,1]} |P(z, p_1, p_2, y)| \\ ||\nabla P|| &= \max_{(\alpha,d)\in\Psi, y\in[0,1]} |\nabla P| \end{aligned}$$

where $|\nabla(\cdot)|$ is the sum of the absolute value of all its first derivatives.

Now we begin estimating $|\tilde{\alpha} - \hat{\alpha}|$ and $|\tilde{d} - \hat{d}|$

$$\begin{aligned} |\tilde{\alpha} - \hat{\alpha}| \leq & \ \textstyle\sum_{j=1}^{4} \int_0^y |F_j(\tilde{\alpha}, \tilde{d}, y) - F_j(\hat{\alpha}, \hat{d}, y)| \, d\tau \\ \leq & \ \textstyle\sum_{j=1}^{4} ||\nabla F_j|| \int_0^y |\tilde{\alpha} - \hat{\alpha}| + |\tilde{d} - \hat{d}| \, d\tau \\ \leq & \ ||\nabla F|| \textstyle\int_0^y |\tilde{\alpha} - \hat{\alpha}| + |\tilde{d} - \hat{d}| \, d\tau \\ |\tilde{d} - \hat{d}| \leq & \ \frac{1}{2} e^{||P||} ||\nabla P|| \int_0^y \left(|\tilde{f} - \hat{f}| + |\tilde{f}_x - \hat{f}_x| + |\tilde{f}_y - \hat{f}_y|\right)\Big|_{(x,y)=(x_1,y)} d\tau. \end{aligned}$$

$|\tilde{f}(x_1,y)-\hat{f}(x_1,y)|$ is further estimated as follows

$$\begin{aligned} & |\tilde{f}(x_1,y)-\hat{f}(x_1,y)| \\ = \; & |\tilde{z}(\tilde{x}_0(x_1,y),y)-\hat{z}(\hat{x}_0(x_1,y),y)| \\ \leq \; & |\tilde{z}(\tilde{x}_0(x_1,y),y)-\tilde{z}(\hat{x}_0(x_1,y),y)|+|\tilde{z}(\hat{x}_0(x_1,y),y)-\hat{z}(\hat{x}_0(x_1,y),y)| \\ \leq \; & ||\tilde{z}_{x_0}|||\tilde{x}_0(x_1,y)-\hat{x}_0(x_1,y)|+|\tilde{z}-\hat{z}|\big|_{\hat{x}_0(x_1,y)}. \end{aligned}$$

Noting

$$\tilde{x}(\tilde{x}_0(x_1,y),y)=\hat{x}(\hat{x}_0(x_1,y),y)=x_1$$

$$\Downarrow$$

$$\begin{aligned} & |\hat{x}(\hat{x}_0(x_1,y),y)-\hat{x}(\tilde{x}_0(x_1,y),y)| \\ = \; & |\tilde{x}(\tilde{x}_0(x_1,y),y)-\hat{x}(\tilde{x}_0(x_1,y),y)| \\ \leq \; & |\tilde{x}-\hat{x}|\big|_{\tilde{x}_0(x_1,y)}, \end{aligned}$$

then

$$\begin{aligned} & |\tilde{x}_0(x_1,y)-\hat{x}_0(x_1,y)| \\ = \; & |\hat{x}_0(\hat{x}(\tilde{x}_0(x_1,y),y),y)-\hat{x}_0(\hat{x}(\hat{x}_0(x_1,y),y),y)| \\ \leq \; & ||\hat{x}_{0x}||\,|\tilde{x}-\hat{x}|\big|_{\tilde{x}_0(x_1,y)}. \end{aligned}$$

Therefore,

$$\begin{aligned} & |\tilde{f}(x_1,y)-\hat{f}(x_1,y)| \\ \leq \; & ||\hat{x}_{0x}||\cdot||\tilde{z}_{x_0}||\cdot|\tilde{x}-\hat{x}|\big|_{\tilde{x}_0(x_1,y)}+|\tilde{z}-\hat{z}|\big|_{\hat{x}_0(x_1,y)}. \end{aligned}$$

Similarly,

$$\begin{aligned}
& |\tilde{f}_x(x_1, y) - \hat{f}_x(x_1, y)| \\
\leq\ & ||\hat{x}_{0x}|| \cdot ||\tilde{p}_{1x_0}|| \cdot |\tilde{x} - \hat{x}|\big|_{\tilde{x}_0(x_1, y)} + |\tilde{p}_1 - \hat{p}_1|\big|_{\hat{x}_0(x_1, y)}, \\
& |\tilde{f}_y(x_1, y) - \hat{f}_y(x_1, y)| \\
\leq\ & ||\hat{x}_{0x}|| \cdot ||\tilde{p}_{2x_0}|| \cdot |\tilde{x} - \hat{x}|\big|_{\tilde{x}_0(x_1, y)} + |\tilde{p}_2 - \hat{p}_2|\big|_{\hat{x}_0(x_1, y)}.
\end{aligned}$$

In summary,

$$\begin{aligned}
& |\tilde{d} - \hat{d}| \\
\leq\ & \frac{1}{2} e^{||P||} ||\nabla P|| (||\hat{x}_{0x}|| \cdot ||\tilde{\alpha}_{x_0}|| + 1) \int_0^y |\tilde{x} - \hat{x}|\big|_{\tilde{x}_0(x_1, \tau)} \\
& + |\tilde{\alpha} - \hat{\alpha}|\big|_{\hat{x}_0(x_1, \tau)}\, d\tau \\
\leq\ & \frac{1}{2} e^{||P||} ||\nabla P|| (||\hat{x}_{0x}|| \cdot ||\tilde{\alpha}_{x_0}|| + 1) \int_0^y |\tilde{\alpha} - \hat{\alpha}|\big|_{\tilde{x}_0(x_1, \tau)} \\
& + |\tilde{\alpha} - \hat{\alpha}|_{\hat{x}_0(x_1, \tau)}\, d\tau.
\end{aligned}$$

Therefore

$$\begin{aligned}
& |\tilde{\alpha} - \hat{\alpha}| + |\tilde{d} - \hat{d}| \\
\leq\ & E\Big(\textstyle\int_0^y |\tilde{\alpha} - \hat{\alpha}|\big|_{x_0} + |\tilde{d} - \hat{d}|\, d\tau + \int_0^y |\tilde{\alpha} - \hat{\alpha}|\big|_{\tilde{x}_0(x_1, \tau)} + |\tilde{d} - \hat{d}|\, d\tau \\
& + \textstyle\int_0^y |\tilde{\alpha} - \hat{\alpha}|\big|_{\hat{x}_0(x_1, \tau)} + |\tilde{d} - \hat{d}|\, d\tau \Big)
\end{aligned}$$

where $E = ||\nabla F|| + \dfrac{1}{2} e^{||P||} ||\nabla P|| (||\hat{x}_{0x}|| \cdot ||\tilde{\alpha}_{x_0}|| + 1)$.

Clearly,

$$|\tilde{\alpha} - \hat{\alpha}| + |\tilde{d} - \hat{d}| \le m$$

hence for any $n \ge 0$

$$|\tilde{\alpha} - \hat{\alpha}| + |\tilde{d} - \hat{d}| \le m(3E)^n \frac{y^n}{n!}\,.$$

Let n approach infinity and we derive

$$\tilde{\alpha} = \hat{\alpha}, \quad \tilde{d} = \hat{d}$$

which implies that

$$\tilde{f}(x,y) \equiv \hat{f}(x,y) \quad \text{in } \Lambda \cap [0,1] \times [0,\theta]\,.$$

Let λ be the largest length such that

$$\tilde{f}(x,y) \equiv \hat{f}(x,y) \quad \text{in } \Lambda \cap [0,1] \times [0,\lambda]\,.$$

If $[0,1] \times (\lambda, 1] \cap \Lambda$ is not empty, we would have a contradiction that there exists $\rho > 0$ such that in $\Lambda \cap [0,1] \times [\lambda, \lambda + \rho]$, $\tilde{f}(x,y) \equiv \hat{f}(x,y)$ by repeating the exact same arguments we have used for proving uniqueness in $[0,\theta]$. Therefore we have

$$\tilde{f}(x,y) = \hat{f}(x,y) \quad \text{in } \Lambda.$$

$\square$

2.3 Numerical Solutions

In the previous section, we establish local existence and uniqueness of the initial value problem of (2.7) and (2.8) with the initial condition (2.9). In this section, we will study the numerical solution of this initial value problem. We propose an algorithm $(**)$ as follows

Step 1. Assign an arbitrary function to d_0 with $d_0(0) = \dfrac{1}{2}$.

Step 2. Substitute d_0 into (2.7) and solve for a numerical solution, namely, f_0.

Step 3. Substitute f_0 into (2.8) and solve for a numerical solution, namely, d_1.

Step 4. Repeat Step 2 and Step 3 to obtain f_i and d_{i+1} until $|d_{i+1} - d_i| < 10^{-4}$.

$$d_i \xrightarrow{\text{Step 2}} f_i \xrightarrow{\text{Step 3}} d_{i+1}$$

Step 5. Substitute the latest d_n into (2.7) and obtain a numerical solution for $f(x, y)$, namely, f_n.

We consider f_n, d_n as the numerical solution of this initial value problem.

2.3.1 Approximation of $f(x, y)$

In Step 2, we consider using the fourth-order Runge-Kutta method (RK4) to solve (2.10)-(2.14) — the system of characteristic ODEs associated with (2.7) — to obtain the approximation of $f(x, y)$. Since the numerical results for $\mathbf{z}, \mathbf{p_1}, \mathbf{p_2}$ are based on a set of scatter points, we consider to do the linear interpolation of these data to approximate $f,\ f_x,\ f_y$ over the regular grids.

2.3.1.1 Numerical Scheme for Characteristic ODEs

The fourth-order Runge-Kutta method for (2.10)- (2.14) is given as

$$
\begin{aligned}
\mathbf{x}_{j+1} &= \mathbf{x}_j + \frac{ds}{6}(XK_1 + 2XK_2 + 2XK_3 + XK_4) \\
\mathbf{y}_{j+1} &= \mathbf{y}_j + \frac{ds}{6}(YK_1 + 2YK_2 + 2YK_3 + YK_4) \\
\mathbf{z}_{j+1} &= \mathbf{z}_j + \frac{ds}{6}(ZK_1 + 2ZK_2 + 2ZK_3 + ZK_4) \\
\mathbf{p_1}_{j+1} &= \mathbf{p_1}_j + \frac{ds}{6}(P_1K_1 + 2P_1K_2 + 2P_1K_3 + P_1K_4) \\
\mathbf{p_2}_{j+2} &= \mathbf{p_2}_j + \frac{ds}{6}(P_2K_2 + 2P_2K_2 + 2P_2K_3 + P_2K_4)
\end{aligned}
$$

with the step size ds and

$$
\begin{aligned}
XK_1 &= X(\mathbf{x}_j, \mathbf{y}_j, \mathbf{z}_j, \mathbf{p_1}_j, \mathbf{p_2}_j) \\
YK_1 &= Y(\mathbf{x}_j, \mathbf{y}_j, \mathbf{z}_j, \mathbf{p_1}_j, \mathbf{p_2}_j) \\
ZK_1 &= Z(\mathbf{x}_j, \mathbf{y}_j, \mathbf{z}_j, \mathbf{p_1}_j, \mathbf{p_2}_j) \\
P_1K_1 &= P_1(\mathbf{x}_j, \mathbf{y}_j, \mathbf{z}_j, \mathbf{p_1}_j, \mathbf{p_2}_j) \\
P_2K_1 &= P_2(\mathbf{x}_j, \mathbf{y}_j, \mathbf{z}_j, \mathbf{p_1}_j, \mathbf{p_2}_j)
\end{aligned}
$$

and

$$
\begin{aligned}
XK_2 &= X(\mathbf{x}_j + \frac{ds}{2}XK_1, \mathbf{y}_j + \frac{ds}{2}YK_1, \mathbf{z}_j + \frac{ds}{2}ZK_1, \mathbf{p_1}_j + \frac{ds}{2}P_1K_1, \mathbf{p_2}_j + \frac{ds}{2}P_2K_1) \\
YK_2 &= Y(\mathbf{x}_j + \frac{ds}{2}XK_1, \mathbf{y}_j + \frac{ds}{2}YK_1, \mathbf{z}_j + \frac{ds}{2}ZK_1, \mathbf{p_1}_j + \frac{ds}{2}P_1K_1, \mathbf{p_2}_j + \frac{ds}{2}P_2K_1) \\
ZK_2 &= Z(\mathbf{x}_j + \frac{ds}{2}XK_1, \mathbf{y}_j + \frac{ds}{2}YK_1, \mathbf{z}_j + \frac{ds}{2}ZK_1, \mathbf{p_1}_j + \frac{ds}{2}P_1K_1, \mathbf{p_2}_j + \frac{ds}{2}P_2K_1) \\
P_1K_2 &= P_1(\mathbf{x}_j + \frac{ds}{2}XK_1, \mathbf{y}_j + \frac{ds}{2}YK_1, \mathbf{z}_j + \frac{ds}{2}ZK_1, \mathbf{p_1}_j + \frac{ds}{2}P_1K_1, \mathbf{p_2}_j + \frac{ds}{2}P_2K_1) \\
P_2K_2 &= P_2(\mathbf{x}_j + \frac{ds}{2}XK_1, \mathbf{y}_j + \frac{ds}{2}YK_1, \mathbf{z}_j + \frac{ds}{2}ZK_1, \mathbf{p_1}_j + \frac{ds}{2}P_1K_1, \mathbf{p_2}_j + \frac{ds}{2}P_2K_1)
\end{aligned}
$$

and

$$
\begin{aligned}
XK_3 &= X(\mathbf{x}_j + \frac{ds}{2}XK_2, \mathbf{y}_j + \frac{ds}{2}YK_2, \mathbf{z}_j + \frac{ds}{2}ZK_2, \mathbf{p_1}_j + \frac{ds}{2}P_1K_2, \mathbf{p_2}_j + \frac{ds}{2}P_2K_2) \\
YK_3 &= Y(\mathbf{x}_j + \frac{ds}{2}XK_2, \mathbf{y}_j + \frac{ds}{2}YK_2, \mathbf{z}_j + \frac{ds}{2}ZK_2, \mathbf{p_1}_j + \frac{ds}{2}P_1K_2, \mathbf{p_2}_j + \frac{ds}{2}P_2K_2) \\
ZK_3 &= Z(\mathbf{x}_j + \frac{ds}{2}XK_2, \mathbf{y}_j + \frac{ds}{2}YK_2, \mathbf{z}_j + \frac{ds}{2}ZK_2, \mathbf{p_1}_j + \frac{ds}{2}P_1K_2, \mathbf{p_2}_j + \frac{ds}{2}P_2K_2) \\
P_1K_3 &= P_1(\mathbf{x}_j + \frac{ds}{2}XK_2, \mathbf{y}_j + \frac{ds}{2}YK_2, \mathbf{z}_j + \frac{ds}{2}ZK_2, \mathbf{p_1}_j + \frac{ds}{2}P_1K_2, \mathbf{p_2}_j + \frac{ds}{2}P_2K_2) \\
P_2K_3 &= P_2(\mathbf{x}_j + \frac{ds}{2}XK_2, \mathbf{y}_j + \frac{ds}{2}YK_2, \mathbf{z}_j + \frac{ds}{2}ZK_2, \mathbf{p_1}_j + \frac{ds}{2}P_1K_2, \mathbf{p_2}_j + \frac{ds}{2}P_2K_2)
\end{aligned}
$$

and

$$
\begin{aligned}
XK_4 &= X(\mathbf{x}_j + dsXK_3, \mathbf{y}_j + dsYK_3, \mathbf{z}_j + dsZK_3, \mathbf{p_1}_j + dsP_1K_3, \mathbf{p_2}_j + dsP_2K_3) \\
YK_4 &= Y(\mathbf{x}_j + dsXK_3, \mathbf{y}_j + dsYK_3, \mathbf{z}_j + dsZK_3, \mathbf{p_1}_j + dsP_1K_3, \mathbf{p_2}_j + dsP_2K_3) \\
ZK_4 &= Z(\mathbf{x}_j + dsXK_3, \mathbf{y}_j + dsYK_3, \mathbf{z}_j + dsZK_3, \mathbf{p_1}_j + dsP_1K_3, \mathbf{p_2}_j + dsP_2K_3) \\
P_1K_4 &= P_1(\mathbf{x}_j + dsXK_3, \mathbf{y}_j + dsYK_3, \mathbf{z}_j + dsZK_3, \mathbf{p_1}_j + dsP_1K_3, \mathbf{p_2}_j + dsP_2K_3) \\
P_2K_4 &= P_2(\mathbf{x}_j + dsXK_3, \mathbf{y}_j + dsYK_3, \mathbf{z}_j + dsZK_3, \mathbf{p_1}_j + dsP_1K_3, \mathbf{p_2}_j + dsP_2K_3).
\end{aligned}
$$

2.3.1.2 Linear Interpolation over Regular Grids

We use RK4 to solve (2.10)-(2.14) with the initial point x_0 from 0.02 to 1 with $\Delta x = 0.02$. We denote the numerical results by $\{x_k,\ y_k,\ z_k,\ p_{1k},\ p_{2k}\}$ with a counting index k. We generate a set of regular grids (X_l, Y_j) by discretizing the xy-plane. To obtain the approximation of $f(x,y)$, $f_x(x,y)$, $f_y(x,y)$ on (X_l, Y_j), we take the following steps

(1) For each grid (X_l, Y_j), we find the three nearest points to it — namely (x_{n1}, y_{n1}), (x_{n2}, y_{n2}) and (x_{n3}, y_{n3}) — from the set of (x_k, y_k) with all k

(2) Do linear interpolation on (x_{n1}, y_{n1}, z_{n1}), (x_{n2}, y_{n2}, z_{n2}) and (x_{n3}, y_{n3}, z_{n3}) to obtain the approximation of $f(X_l, Y_j)$

(3) Do linear interpolation on $(x_{n1}, y_{n1}, p_{1n1})$, $(x_{n2}, y_{n2}, p_{1n2})$ and $(x_{n3}, y_{n3}, p_{1n3})$ to obtain the approximation of $f_x(X_l, Y_j)$

(4) Do linear interpolation on $(x_{n1}, y_{n1}, p_{2n1})$, $(x_{n2}, y_{n2}, p_{2n2})$ and $(x_{n3}, y_{n3}, p_{2n3})$ to obtain the approximation of $f_y(X_l, Y_j)$.

2.3.2 Approximation of $d(y)$

From (2.8), $d(y)$ can be explicitly solved as

$$d(y) = \frac{1}{2}\, e^{-\int_0^y P(x_1,\tau)\, d\tau}$$

where

$$P(x_1,\tau) = \frac{2x_1^2 f_x(x_1,\tau) + 4x_1 f(x_1,\tau) - 2\displaystyle\int_0^\tau \frac{c_x(x_1,t)}{c^2(x_1,t)}\, dt}{x_1^3 f_y(x_1,\tau) + \dfrac{x_1}{c(x_1,\tau)}}.$$

Assume $\{(X_\rho, Y_j)\}$ is a set of regular grids on the line $\{x = x_1\}$ where $Y_j = (j-1)\Delta y$ with positive integer j and spacing Δy. We use the composite Simpson's rule to approximate $d(y)$:

(1) Evaluate $d(y)$ at the odd grids $\{Y_3, Y_5, Y_7 \cdots\}$ using the scheme

$$d(Y_k) = \frac{1}{2}\exp(-\sum_{j=1}^{k-2}\int_{Y_j}^{Y_{j+2}} P(x_0,\tau)\, d\tau)$$

where

$$\int_{Y_j}^{Y_{j+2}} P(x_0,\tau)\, d\tau \approx \frac{\Delta y}{3}\big(P(x_1,Y_j) + 4P(x_1,Y_{j+1}) + P(x_1,Y_{j+2})\big).$$

(2) Evaluate $d(Y_2)$ using the rectangle method

$$\int_0^{Y_2} P(x_0,\tau)\, d\tau \approx \Delta y P(x_1,\Delta y)\,.$$

Evaluate $d(Y_k)$ at the even grids $\{Y_4, Y_6, Y_8 \cdots\}$ using the scheme

$$d(Y_k) = \frac{1}{2}\exp(-\int_0^{Y_2} P(x_0,\tau)\, d\tau - \sum_{j=2}^{k-2}\int_{Y_j}^{Y_{j+2}} P(x_0,\tau)\, d\tau)$$

where

$$\int_{Y_j}^{Y_{j+2}} P(x_0,\tau)\,d\tau \approx \frac{\Delta y}{3}\big(P(x_1,Y_j)+4P(x_1,Y_{j+1})+P(x_1,Y_{j+2})\big).$$

(3) Do linear interpolation between $(Y_j, d(Y_j))$ and $(Y_{j+1}, d(Y_{j+1}))$ to approximate $d(y)$ on every subinterval $[Y_j, Y_{j+1}]$.

2.3.3 Numerical Examples

We implement the algorithm $(**)$ over the domain $[0.1,1]\times[0,2]$ in the following three media

1. C_1 is a homogeneous medium with $c(x,y)\equiv 1$.

2. C_2 is an inhomogeneous medium with $c(x,y)$ defined as

$$\begin{cases} 1-8(\dfrac{(x-2)^2}{4}+4(y-1)^2-\dfrac{1}{4})^2 & \text{if } \dfrac{(x-2)^2}{2}+4(y-1)^2\le\dfrac{1}{4} \\ & \quad\text{and } x\ge 2\,; \\ 1-8(\dfrac{(x+2)^2}{4}+4(y-1)^2-\dfrac{1}{4})^2 & \text{if } \dfrac{(x+2)^2}{4}+4(y-1)^2\le\dfrac{1}{4} \\ & \quad\text{and } x\le -2\,; \\ 1-8(4(y-1)^2-\dfrac{1}{4})^2 & \text{if } \dfrac{3}{4}\le y\le\dfrac{5}{4} \text{ and } -2<x<2; \\ 1 & \text{everywhere else.} \end{cases}$$

Figure 2.1: The medium C_2

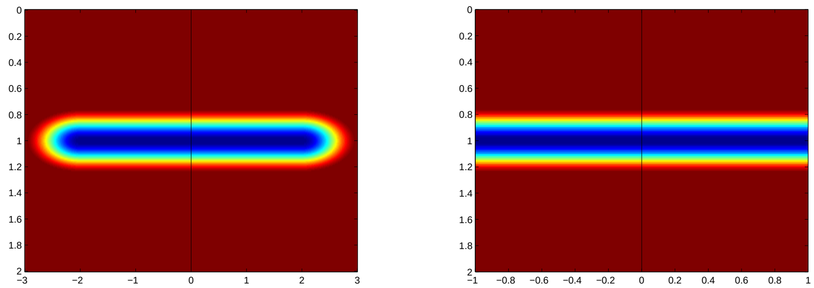

(a) Over the domain $[-3,3]\times[0,2]$ (b) Over the domain $[-1,1]\times[0,2]$

3. C_3 is an inhomogeneous medium with $c(x,y)$ defined as

$$\begin{cases} 1-8[\dfrac{(x-1.1)^2}{4}+4(y-\dfrac{1}{2})^2-\dfrac{1}{4}]^2 & \text{if } \dfrac{(x-1.1)^2}{4}+4(y-\dfrac{1}{2})^2\leq\dfrac{1}{4} \\ & \quad\text{and } 0\leq y\leq\dfrac{1}{2}\,; \\ 1-8[\dfrac{(x-1.1)^2}{4}-\dfrac{1}{4}]^2 & \text{if } \ 0.1\leq x\leq 2.1 \text{ and } y>\dfrac{1}{2}\,; \\ 1 & \text{everywhere else.} \end{cases}$$

Figure 2.2: The medium C_3

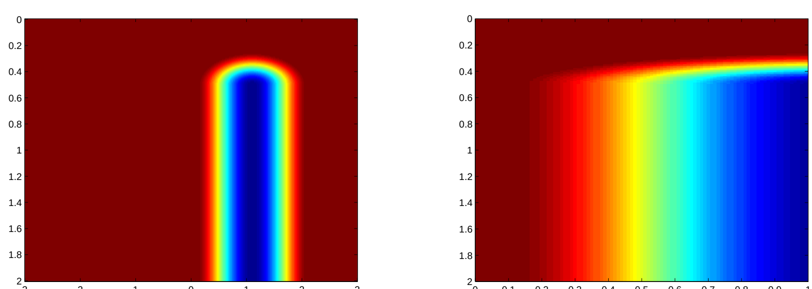

(a) Over the domain $[-3,3]\times[0,2]$ (b) Over the domain $[0,1]\times[0,2]$

2.3.3.1 Simulation in the medium C_1

Let $d_0 = \dfrac{1}{2}$. The characteristic curves for f_0 are shown below

Figure 2.3: The characteristic curves with initial points from 0.02 to 1 with $\Delta x = 0.02$ and the y coordinate restricted within $[0, 2.4]$

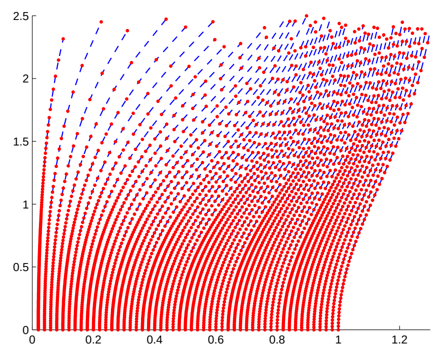

(a) Overview

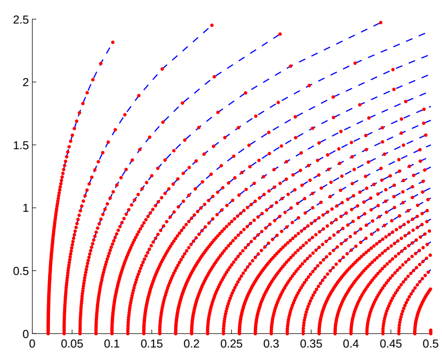

(b) Close-up in $[0, 0.5] \times [0, 2.5]$

The pattern exhibited by all the characteristic curves in Figure 2.3 indicates that we only need to compute the characteristic curve with the initial point x_0 less than $x_1 + \Delta x$ in later iteration until $\max |d_{n+1} - d_n| < 10^{-4}$. Let

$x_1 = 0.25$. After 5 iterations, $\max|d_5 - d_4|$ drops below 10^{-4}. We compare d_{n+1} with d_n after each iteration and the results are listed below

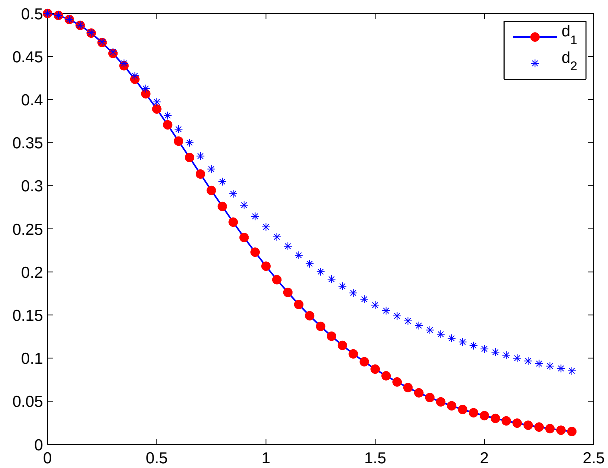

Figure 2.4: $\max\limits_{y\in[0,2.4]} |d_2 - d_1| = 0.0785$

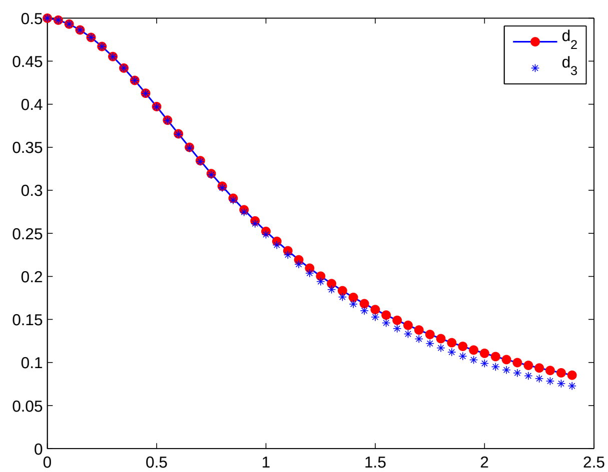

Figure 2.5: $\max\limits_{y\in[0,2.4]} |d_3 - d_2| = 0.0125$

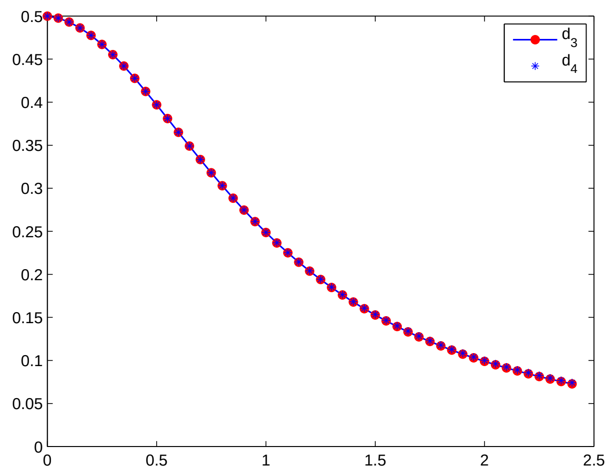

Figure 2.6: $\max_{y\in[0,2.4]} |d_4 - d_3| = 0.0013$

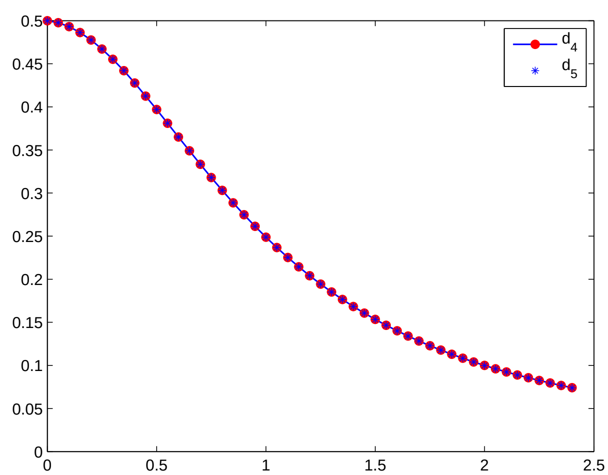

Figure 2.7: $\max_{y\in[0,2.4]} |d_5 - d_4| = 8.6 \times 10^{-5}$

We use d_5 as the approximation of $d(y)$ in (2.7) to approximate $f(x, y)$

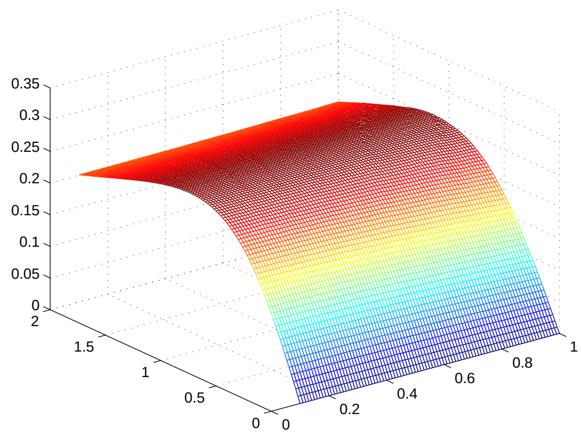

Figure 2.8: The approximation of $f(x, y)$

Finally, we check whether different values of x_1 would have any effect on the value of $d(y)$. We compute d_5 with the approximation of f_4 along two other lines $\{x = 0.11\}$ $\{x = 0.39\}$ and compare them to d_5 with $x_1 = 0.25$.

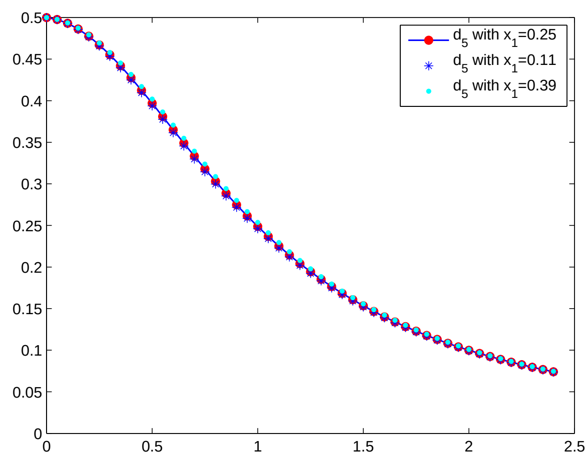

The maximum distance between d_5 with $x_1 = 0.11$ and $x_1 = 0.25$ is 0.0035.

The maximum distance between d_5 with $x_1 = 0.25$ and $x_1 = 0.39$ is 0.0058.

The maximum distance between d_5 with $x_1 = 0.11$ and $x_1 = 0.39$ is 0.0093.

2.3.3.2 Simulation in the medium C_2

We use d_5 — the approximation of $d(y)$ in the medium C_1 shown in Figure 2.7 — as the initial guess for d_0 to approximate f_0. The characteristic curves for f_0 are shown below

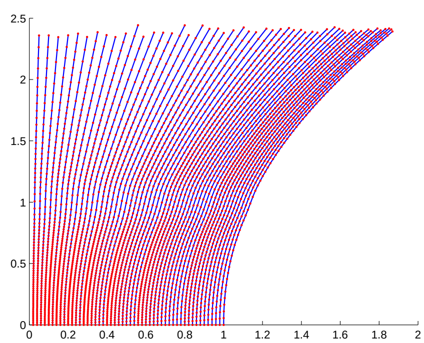

(a) Overview

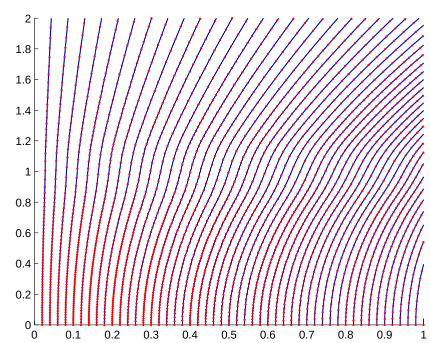

(b) Close-up in $[0, 1] \times [0, 2]$

Figure 2.9: The characteristic curves with initial points from 0.02 to 1 with $\Delta x = 0.02$ and the y coordinate restricted within $[0, 2.4]$

Let $x_1 = 0.5$. We continue the iterations until $\max |d_4 - d_3|$ drops below 10^{-4}. We compare d_{n+1} with d_n after each iteration and the results are listed below

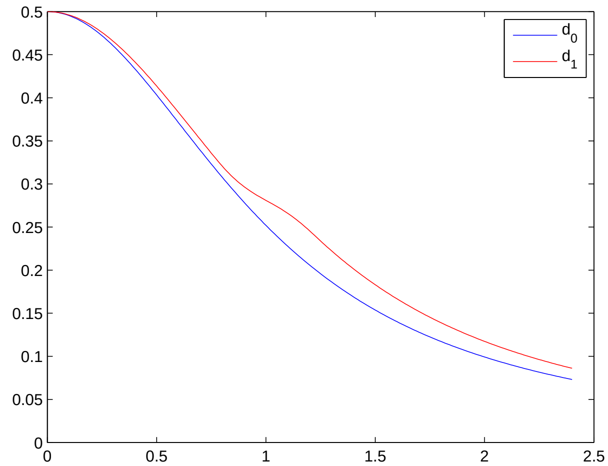

Figure 2.10: $\max_{y\in[0,2.4]} |d_1 - d_0| = 0.0401$

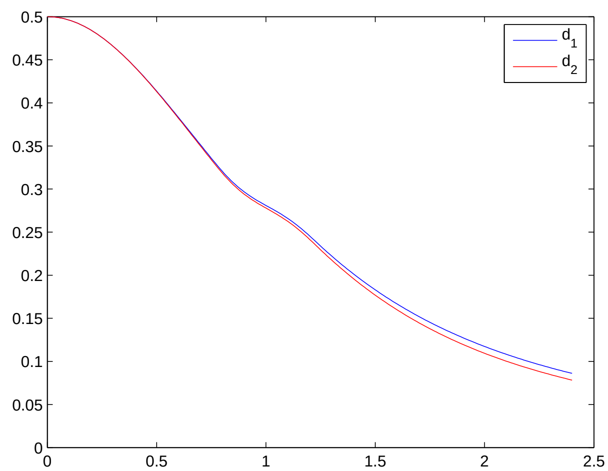

Figure 2.11: $\max_{y\in[0,2.4]} |d_2 - d_1| = 0.0080$

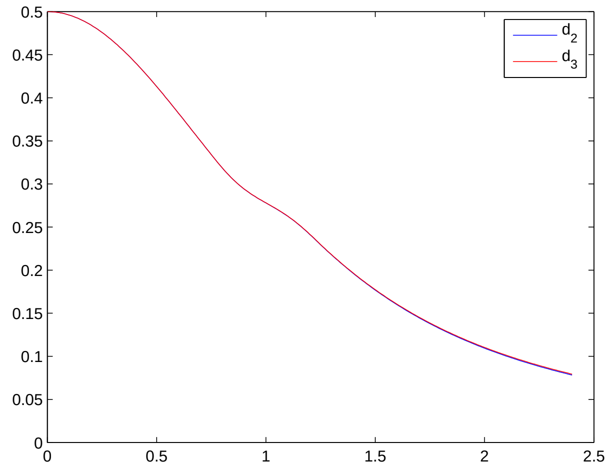

Figure 2.12: $\max_{y\in[0,2.4]} |d_3 - d_2| = 0.0011$

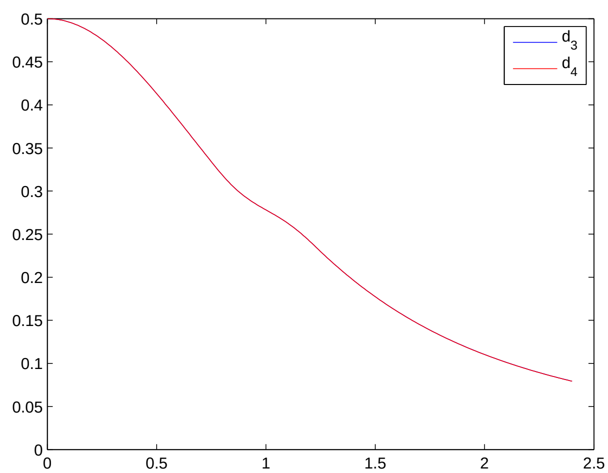

Figure 2.13: $\max_{y\in[0,2.4]} |d_4 - d_3| = 7.9 \times 10^{-5}$

We use d_4 as the approximation of $d(y)$ in (2.7) to simulate $f(x, y)$

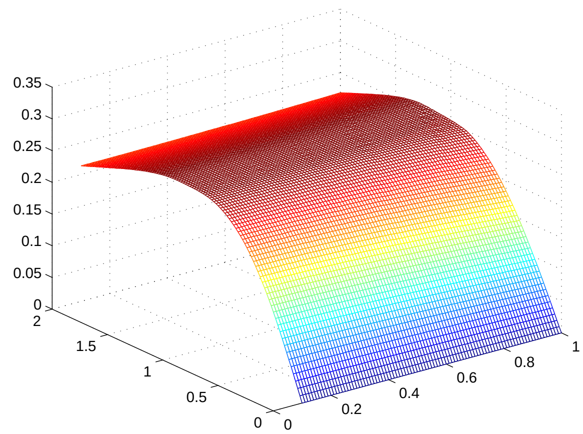

Figure 2.14: The approximation of $f(x, y)$

In the end, we compute d_4 with the approximation of f_3 along two other lines $\{x = 0.4\}$ $\{x = 0.6\}$ and compare them to d_4 with $x_1 = 0.5$.

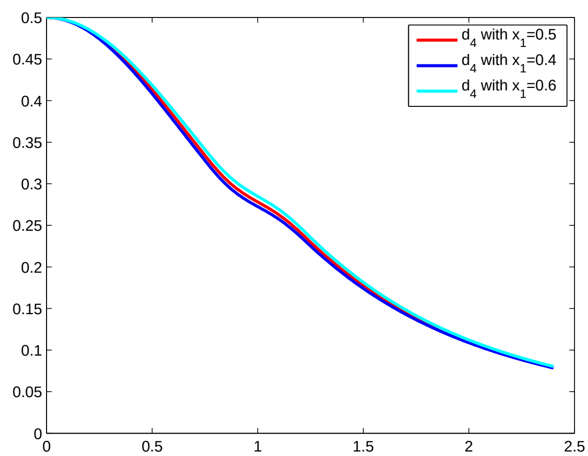

The maximum distance between d_4 with $x_1 = 0.5$ and $x_1 = 0.4$ is 0.0061.

The maximum distance between d_4 with $x_1 = 0.5$ and $x_1 = 0.6$ is 0.0073.

The maximum distance between d_4 with $x_1 = 0.4$ and $x_1 = 0.6$ is 0.0134.

2.3.3.3 Simulation in the medium C_3

We use d_5 — the approximation of $d(y)$ in the medium C_1 shown in Figure 2.7 — as the initial guess for d_0 to approximate f_0. The characteristic curves for f_0 are shown below

Figure 2.15: The characteristic curves with initial points from 0.005 to 1 with $\Delta x = 0.005$ and the y coordinate restricted within $[0, 2.4]$

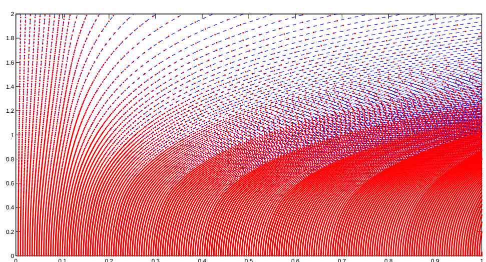

(a) Overview

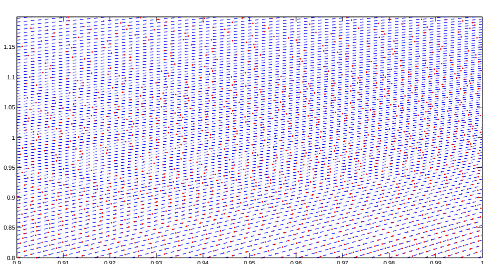

(b) Close-up in $[0.9, 1] \times [0.8, 1.2]$

Let $x_1 = 0.5$. We continue the iterations until $\max|d_3 - d_2|$ drops below 10^{-4}. We compare d_{n+1} with d_n after each iteration with the results listed below

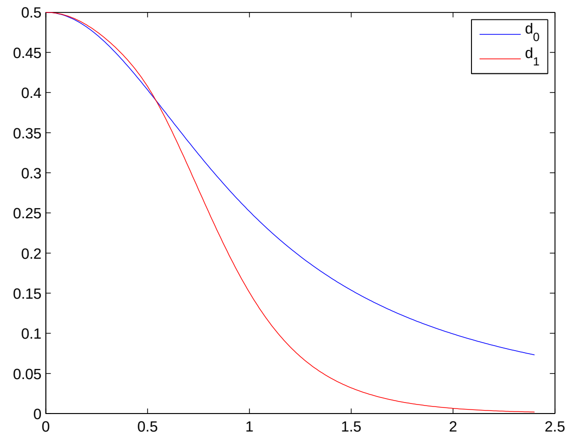

Figure 2.16: $\max_{y\in[0,2.4]} |d_1 - d_0| = 0.1257$

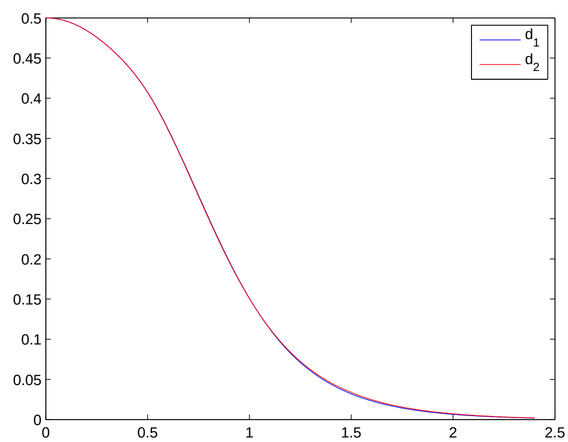

Figure 2.17: $\max_{y\in[0,2.4]} |d_2 - d_1| = 0.0018$

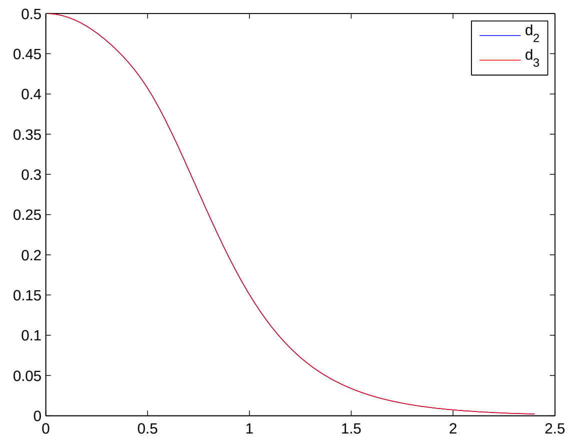

Figure 2.18: $\max_{y \in [0,2.4]} |d_3 - d_2| = 5.7 \times 10^{-5}$

We use d_3 as the approximation of $d(y)$ in (2.7) to simulate $f(x, y)$

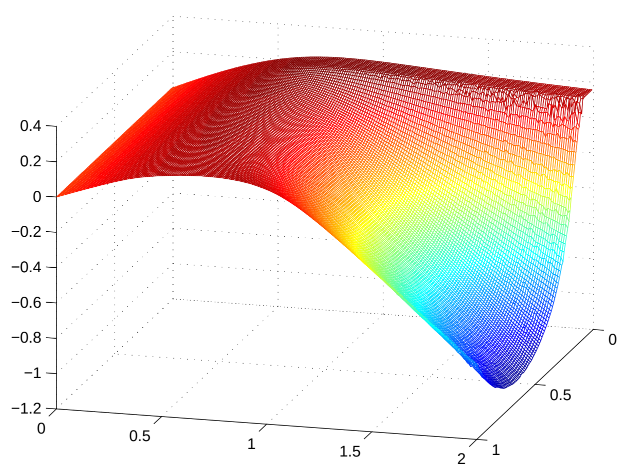

Figure 2.19: The approximation of $f(x, y)$ in $[0.1, 1] \times [0, 2]$

We also compute d_3 with the approximation of f_2 along two other lines $\{x = 0.4\}$ $\{x = 0.6\}$ and compare them to d_3 with $x_1 = 0.5$.

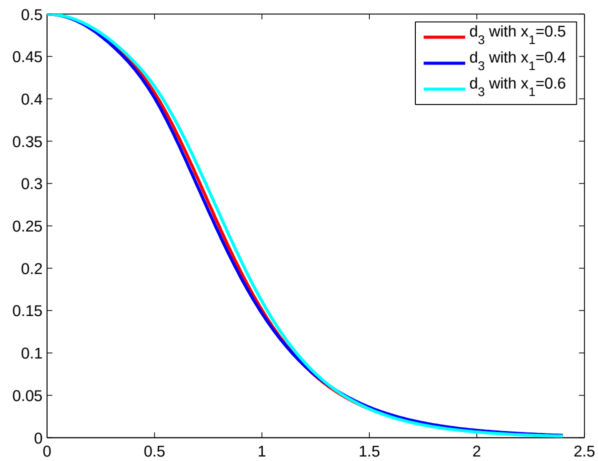

The maximum distance between d_3 with $x_1 = 0.5$ and $x_1 = 0.4$ is 0.0098.

The maximum distance between d_3 with $x_1 = 0.5$ and $x_1 = 0.6$ is 0.0155.

The maximum distance between d_3 with $x_1 = 0.4$ and $x_1 = 0.6$ is 0.0250.

Chapter 3

The Wave Model and its Simulation

We assume that the wave has the form $A(x,y)e^{i\omega(a(x,y)+ib(x,y))}$ which is equivalent to $\boxed{A(x,y)e^{-\omega b(x,y)}}\,e^{i\omega\boxed{a(x,y)}}$. We expect the amplitude $A(x,y)e^{-\omega b(x,y)}$ and the phase $a(x,y)$ to satisfy the transport equation

$$2\nabla a(x,y)\cdot\nabla\big(A(x,y)e^{-\omega b(x,y)}\big)+A(x,y)e^{-\omega b(x,y)}\Delta a(x,y)=0$$

which is equivalent to

$$2a_xA_x+2a_yA_y+\big(\Delta a-2\omega(a_xb_x+a_yb_y)\big)A=0.$$

Due to $a_xb_x+a_yb_y=0$, we derive an equation for the amplitude $A(x,y)$

$$2a_xA_x+2a_yA_y+\Delta aA=0 \tag{3.1}$$

where the coefficients a_x, a_y and Δa are explicitly given as

$$\begin{aligned}
a_x &= \textstyle\int_0^y(\frac{1}{c})_x\,ds+2xf(x,y)+x^2f_x\\
a_y &= \frac{1}{c}+x^2f_y\\
a_{xx} &= \textstyle\int_0^y(\frac{1}{c})_{xx}\,ds+2f+4xf_x+x^2f_{xx}\\
a_{yy} &= (\frac{1}{c})_y+x^2f_{yy}.
\end{aligned}$$

Its boundary condition is given as $A(x,0)=1$ because we would like the wave to have a standard Gaussian profile $e^{-\frac{1}{2}x^2}$ on the x-axis.

Our ultimate goal in this section is to simulate this wave in the domain $[-1,1]\times[0,2]$. Apparently, we need to first have the approximation of $f(x,y)$ in this domain. We already have local existence and uniqueness of the initial value problem of $f(x,y)$ and $d(y)$ inside the domain $[\delta,1]\times[0,2]$ with any small $\delta>0$. Similarly, we can establish the same results inside the domain $[-1,-\delta]\times[0,2]$ due to the fact that $F_{p_2}(x_0,0,0,0,f_y(x_0,0))\neq 0$ holds in $[-1,0)$. Since δ is as small as we wish, we only need to find $f(x,y)$ on the y-axis.

3.1 ODE for $f(0,y)$

By performing the degeneracy analysis on (2.5), we can obtain an ordinary differential equation for $f(0,y)$. Recall (2.5)

$$x^4(f_x^2+f_y^2)+(4x^3f-2x^2\int_0^y \frac{c_x}{c^2}ds)f_x+\frac{2x^2}{c}f_y+4x^2f^2-4x(\int_0^y \frac{c_x}{c^2}ds)f$$

$$-x^4d'^2(y)-4x^2d^2(y)+(\int_0^y \frac{c_x}{c^2}ds)^2=0.$$

Divide it by x^2,

$$x^2(f_x^2+f_y^2)+(4xf-2\int_0^y \frac{c_x}{c^2}ds)f_x+\frac{2}{c}f_y+4f^2-4\frac{\int_0^y \frac{c_x}{c^2}ds}{x}f$$

$$-x^2d'^2(y)-4d^2(y)+(\frac{\int_0^y \frac{c_x}{c^2}ds}{x})^2=0.$$

Let x approach 0,

$$\frac{2}{c}f_y(0,y)+4f^2(0,y)-4\lim_{x\to 0}\frac{\int_0^y \frac{c_x}{c^2}ds}{x}f(0,y)-4d^2(y)+(\lim_{x\to 0}\frac{\int_0^y \frac{c_x}{c^2}ds}{x})^2=0.$$

If $\lim_{x\to 0}\frac{\int_0^y \frac{c_x(x,s)}{c^2(x,s)}ds}{x}$ exists, we can derive an ODE for $f(0,y)$

$$f_y(0,y)=2d^2(y)c(0,y)-2c(0,y)\big(f(0,y)-\lim_{x\to 0}\frac{\int_0^y \frac{c_x(x,s)}{c^2(x,s)}ds}{2x}\big)^2.$$

If $c(x,y)$ is C^2

$$\lim_{x\to 0}\frac{\frac{c_x(x,s)}{c^2(x,s)}}{x}=\lim_{x\to 0}\frac{\frac{c_x(x,s)}{c^2(x,s)}-\frac{c_x(0,s)}{c^2(0,s)}}{x}=(\frac{c_x(x,s)}{c^2(x,s)})_x|_{x=0}=\frac{c_{xx}(0,s)}{c^2(0,s)}.$$

By Lebesque's dominated convergence theorem,

$$\lim_{x\to 0}\frac{\int_0^y \frac{c_x(x,s)}{c^2(x,s)}ds}{2x}=\int_0^y \lim_{x\to 0}\frac{\frac{c_x(x,s)}{c^2(x,s)}}{2x}ds=\int_0^y \frac{c_{xx}(0,s)}{2c^2(0,s)}ds.$$

Therefore,

$$f_y(0,y)=2d^2(y)c(0,y)-2c(0,y)\big(f(0,y)-\int_0^y \frac{c_{xx}(0,s)}{2c^2(0,s)}\,ds\big)^2. \tag{3.2}$$

Moreover, if $c_{xx}(0,y)=0$, we have a simple version

$$f_y(0,y)=2c(0,y)(\,d^2(y)-f^2(0,y)\,)\,.$$

(3.2) can be numerically solved by the fourth order Runge-Kutta method. For simplicity, we use the simple version to show its numerical scheme given as follows

$$f(0,y_{j+1})=f(0,y_j)+\frac{\Delta y}{6}\big(k_1+2k_2+2k_3+k_4\big)$$

where $\{(0, y_j)\}$ is a set of equally spaced grids on the y-axis with spacing Δy and

$$\begin{aligned} k_1 &= 2c(0, y_j)(d^2(y_j) - f^2(0, y_j)) \\ k_2 &= 2c(0, y_j + \frac{\Delta y}{2})(d^2(y_j + \frac{\Delta y}{2}) - (f(0, y_j) + k_1 \frac{\Delta y}{2})^2) \\ k_3 &= 2c(0, y_j + \frac{\Delta y}{2})(d^2(y_j + \frac{\Delta y}{2}) - (f(0, y_j) + k_2 \frac{\Delta y}{2})^2) \\ k_4 &= 2c(0, y_{j+1})(d^2(y_{j+1}) - (f(0, y_j) + k_3 \Delta y)^2). \end{aligned}$$

3.2 Approximation of $f(x, y)$ in $[-1, 1] \times [0, 2]$

Due to $c_x(0, y) = 0$, the central ray starting from the origin is traveling strictly downwards along the y-axis. In light of this, we consider breaking the wave into two parts — a left wing in the left-half domain $[-1, 0) \times [0, 2]$ and a right wing in the right-half domain $(0, 1] \times [0, 2]$, and to simulate $f(x, y)$ in each domain respectively. Based on the theoretical and numerical results in Chapter 2, we propose an algorithm for the approximation of $f(x, y)$ in the domain $[-1, 1] \times [0, 2]$ as follows

Step 1. Simulation in the left-half domain $[-1, 0) \times [0, 2]$.

Let $x_1 = x_L$ where x_L is a constant of our choice in $[-1, 0)$. Continue the iteration process until $\max |d_{n+1} - d_n| < 10^{-4}$ for some n. Denote d_{n+1} by d_L. Use d_L as the approximation of $d(y)$ to calculate all the characteristics of $f(x, y)$ with initial points from -0.02 to -1 with 0.02 spacing. This set of characteristics is denoted by $\{x_l,\ y_l,\ z_l,\ p_{1l},\ p_{2l}\}$ with negative counting index $l = -1, -2, -3$ etc.

Step 2. Simulation in the right-half domain $(0,1] \times [0,2]$.

Let $x_1 = x_R$ where x_R is a constant of our choice in $(0,1]$. Continue the iteration process until $\max |d_{n+1} - d_n| < 10^{-4}$ for some n. Denote d_{n+1} by d_R. Use d_R as the approximation of $d(y)$ to calculate all the characteristics of $f(x,y)$ with initial points from 0.02 to 1 with 0.02 spacing. This set of characteristics is denoted by $\{x_r,\, y_r,\, z_r,\, p_{1r},\, p_{2r}\}$ with positive counting index $r = 1, 2, 3$ etc.

Step 3. Approximation of $f(x,y), f_x(x,y), f_y(x,y)$ along the y-axis.

We would like to use (3.2) to approximate $f(0,y)$ and $f_y(0,y)$ but the problem here is which function, d_L or d_R, we should pick for $d(y)$. In the derivation of (3.2), we take the limit as x approaches 0 from both sides. But in reality, we have local existence and uniqueness of $f(x,y)$ and $d(y)$ inside the left- and right-half domain — $[-1,0) \times [0,2]$ and $(0,1] \times [0,2]$ — respectively. Thus if d_L and d_R are different, we will have two different ODEs for $f(0,y)$ by taking the left- and right-hand limits as x approaches 0

$$f_y(0,y) = 2d_L^2 c(0,y) - 2c(0,y)\big(f(0,y) - \lim_{x \to 0^-} \frac{\displaystyle\int_0^y \frac{c_x(x,s)}{c^2(x,s)} ds}{2x}\big)^2$$

$$f_y(0,y) = 2d_R^2 c(0,y) - 2c(0,y)\big(f(0,y) - \lim_{x \to 0^+} \frac{\displaystyle\int_0^y \frac{c_x(x,s)}{c^2(x,s)} ds}{2x}\big)^2.$$

If $d_L \neq d_R$, we skip this step and directly go to the next. If $d_L = d_R$, we first apply the RK4 on (3.2) to approximate $f(0, y_j)$ and $f_y(0, y_j)$. Secondly, we find the approximation of $f_x(0, y_j)$ by doing the linear interpolation on the two closest characteristic curves to the y-axis. The characteristic curve with initial point $x_0 = -0.02$ is the closest to the y-axis from the left-hand side and we denote this curve by (x_l, y_l) with $l \in S_L$ for some set $S_L \subset \mathbb{N}^-$. Similarly, the one with initial point $x_0 = 0.02$ is the closest to the y-axis from the right-hand side and we denote it by (x_r, y_r) with $r \in S_R$ for some subset $S_R \subset \mathbb{N}^+$. For each grid $(0, y_j)$, we find the three nearest points to it, namely (x_{n1}, y_{n1}), (x_{n2}, y_{n2}) and (x_{n3}, y_{n3}), from the set of $\{(x_k, y_k),\ k \in S_L \cup S_R\}$ and do the linear interpolation on $(x_{n1}, y_{n1}, p_{1_{n1}})$, $(x_{n2}, y_{n2}, p_{1_{n2}})$ and $(x_{n3}, y_{n3}, p_{1_{n3}})$ to obtain the approximation of $f_x(0, y_j)$.

Step 4. Approximation of $f(x, y)$ on regular grids in $[-1, 1] \times [0, 2]$.

Consider the following regular grids in $[-1, 1] \times [0, 2]$

$$\{\, (x_j, y_n),\ x_j = j\Delta x,\ y_n = n\Delta y \,\}$$

where

$$j = -\frac{1}{\Delta x}, \cdots, -1, 0, 1, \cdots, \frac{1}{\Delta x};\ n = 0, 1, 2, \cdots, \frac{2}{\Delta y}\,.$$

We break into two cases

(a) If $d_L = d_R$

At each (x_j, y_n) with $x_j \neq 0$, we repeat the same steps in Sub-subsection 2.3.1.2 to approximate $f(x_j, y_n)$, $f_x(x_j, y_n)$ and

$f_y(x_j, y_n)$ from the characteristic union of $\{x_l, y_l, z_l, p_{1l}, p_{2l}\}$, $\{0, y_j, f(0, y_j), f_x(0, y_j), f_y(0, y_j)\}$, and $\{x_r, y_r, z_r, p_{1r}, p_{2r}\}$.

(b) If $d_L \neq d_R$

At each (x_j, y_n), we repeat the same steps in Sub-subsection 2.3.1.2 to approximate $f(x_j, y_n)$, $f_x(x_j, y_n)$ and $f_y(x_j, y_n)$ from the characteristic set of $\{x_l, y_l, z_l, p_{1l}, p_{2l}\}$ and $\{x_r, y_r, z_r, p_{1r}, p_{2r}\}$.

3.3 Approximation of $A(x, y)$

We consider using the Lax-Friedrichs method to solve (3.1). First we rewrite (3.1) into

$$A_y = -\frac{a_x}{a_y} A_x - \frac{\Delta a}{2a_y} A. \tag{3.3}$$

We use A_j^n to denote the approximation of A at (x_j, y_n). The numerical scheme is given as

$$\frac{A_j^{n+1} - \frac{1}{2}(A_{j+1}^n + A_{j-1}^n)}{\Delta y} = -\frac{(a_x)_j^n}{(a_y)_j^n} \frac{A_{j+1}^n - A_{j-1}^n}{2\Delta x} - \frac{(\Delta a)_j^n}{2(a_y)_j^n} A_j^n$$

or solving for A_j^{n+1}

$$A_j^{n+1} = \frac{1}{2}(A_{j+1}^n + A_{j-1}^n) - \frac{(a_x)_j^n \Delta y}{2(a_y)_j^n \Delta x}(A_{j+1}^n - A_{j-1}^n) - \frac{(\Delta a)_j^n \Delta y}{2(a_y)_j^n} A_j^n$$

with the initial condition $A_j^0 = 1$. Its stability condition is

$$\left|\frac{a_x}{a_y} \frac{\Delta y}{\Delta x}\right| \leq 1 \quad \text{or} \quad \left|\frac{a_x}{a_y} \Delta y\right| \leq \Delta x$$

from which, we derive a restrictive condition on Δx with given Δy

$$\max_{j,n} \left|\frac{a_x(x_j, y_n)}{a_y(x_j, y_n)} \Delta y\right| \leq \Delta x.$$

3.4 Numerical Examples

In this section, we implement the algorithm in Section 3.2 and the numerical method in Section 3.3 to approximate $f(x, y)$ and $A(x, y)$ in the domain $[-1, 1] \times [0, 2]$, and then use these results to simulate the wave by the following formula

$$A(x, y)e^{i\omega(a(x,y) + ib(x,y))}$$

where

$$a(x, y) = \int_0^y \frac{1}{c(x, s)} ds + x^2 f(x, y)$$

$$b(x, y) = \begin{cases} x^2 d_L(y) & \text{if} \quad x < 0 \\ 0 & \text{if} \quad x = 0 \\ x^2 d_R(y) & \text{if} \quad x > 0 \end{cases} .$$

We will do the implementation in various media and all the simulations will be done with $\omega = 15$.

Simulation in the medium C_1

C_1 is a homogeneous medium hence we assume $d_L = d_R = d_5$ where d_5 is the approximation of $d(y)$ in the medium C_1, as shown in Figure 2.7. The simulation results are shown below

Figure 3.1: The approximation of $f(x, y)$ in $[-1, 1] \times [0, 2]$

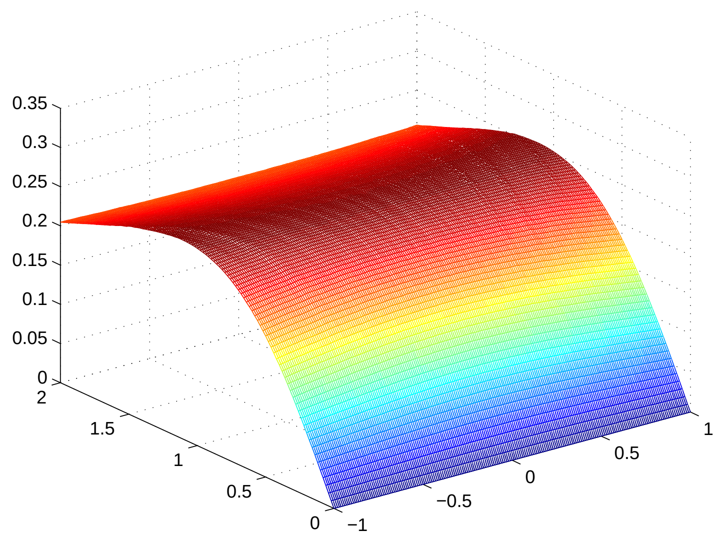

Figure 3.2: The approximation of $A(x, y)$ in $[-1, 1] \times [0, 2]$

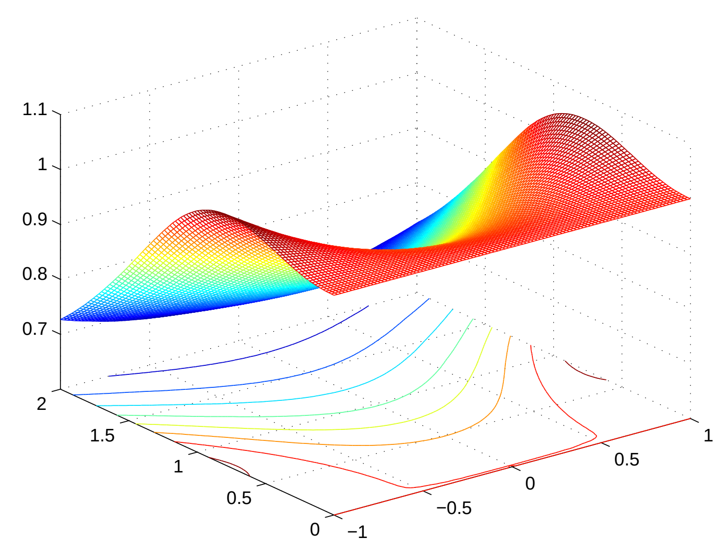

Figure 3.3: The real-part wave $Ae^{-\omega b}\cos(\omega a)$ in $[-1, 1] \times [0, 2]$

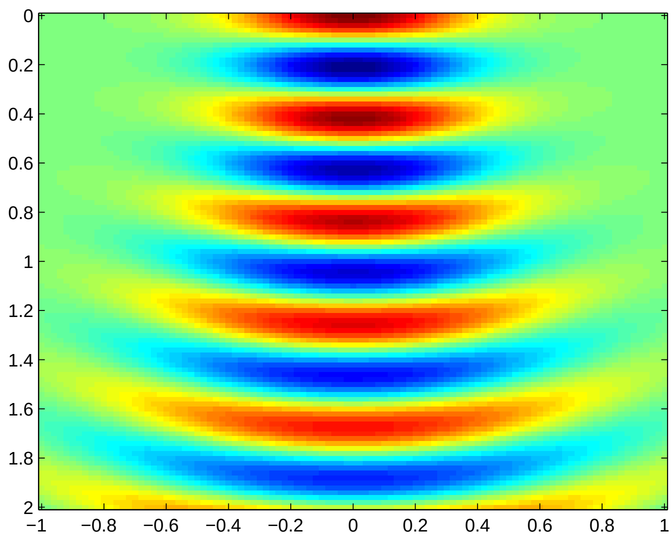

(a) Imagesc picture

Simulation in the medium C_2

The medium C_2 does not depend on x over the domain $[-2, 2] \times [0, 2]$ hence we assume $d_L = d_R = d_4$ where d_4 is the approximation of $d(y)$ in the medium C_2, as shown in Figure 2.13. The simulation results are shown below

Figure 3.4: The approximation of $f(x, y)$ in $[-1, 1] \times [0, 2]$

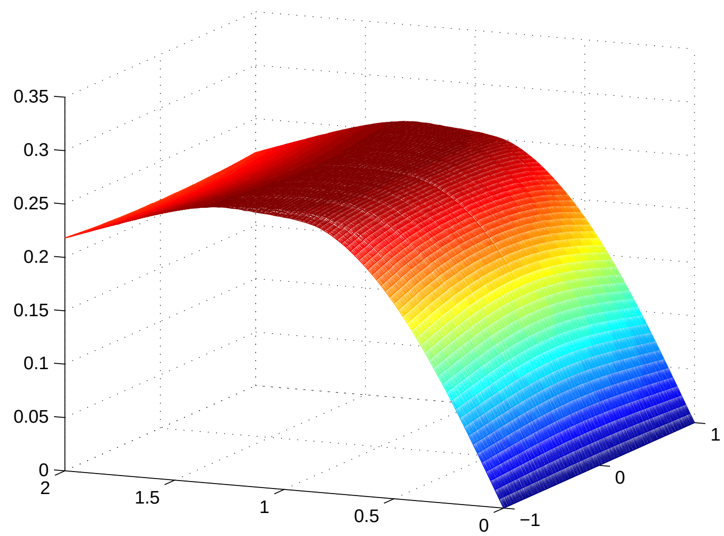

Figure 3.5: The approximation of $A(x, y)$ in $[-1, 1] \times [0, 2]$

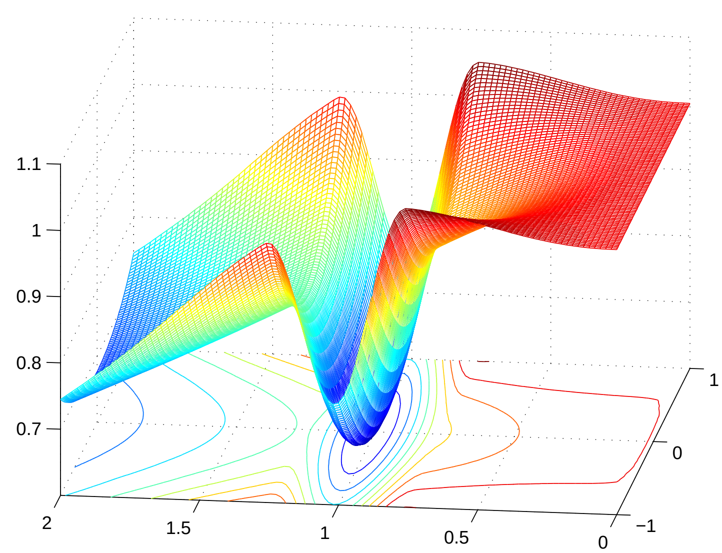

Figure 3.6: The real-part wave $Ae^{-\omega b}\cos(\omega a)$ in $[-1,1]\times[0,2]$

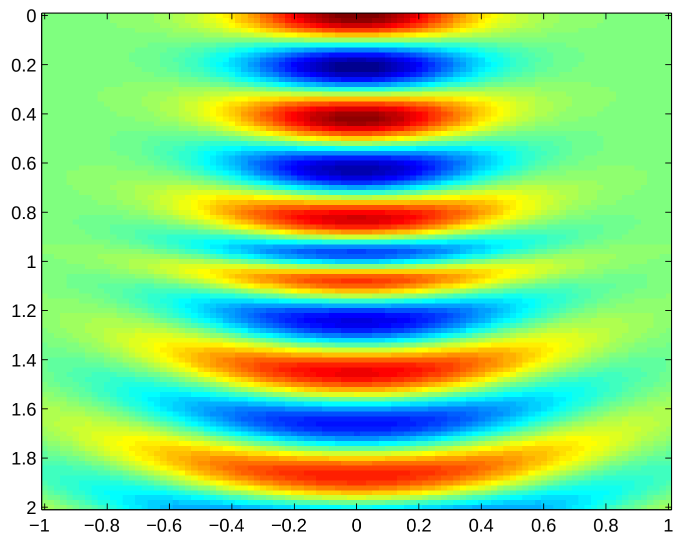

(a) Imagesc picture

In the end, we compare this imagesc picture with the one in the medium C_1 to have a better understanding about this wave

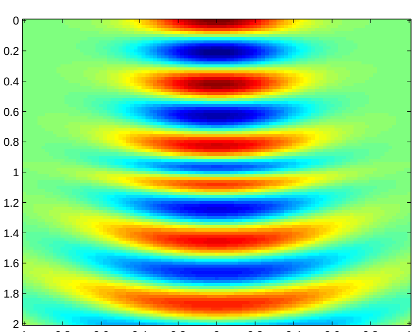

(b) The real-part wave in $\mathbf{C_2}$

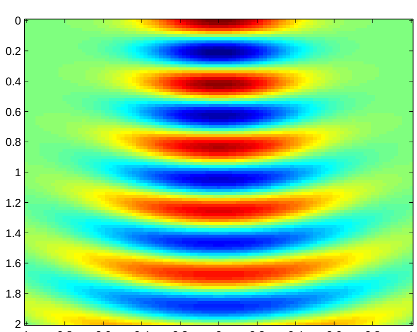

(c) The real-part wave in $\mathbf{C_1}$

Simulation in the medium C_3

Noticing that C_3 is homogeneous with $c(x, y) = 1$ in the left-half plane, we assume $d_L = d_5$ where d_5 is the approximation of $d(y)$ in the medium C_1, as shown in Figure 2.7. Let $d_R = d_3$ where d_3, shown in Figure 2.18, is the approximation of $d(y)$ used to simulate $f(x, y)$ over the domain $[0.1, 1] \times [0, 2]$ in the medium C_3. The simulation results are shown below.

Figure 3.7: The approximation of $f(x, y)$ in $[-1, 1] \times [0, 2]$

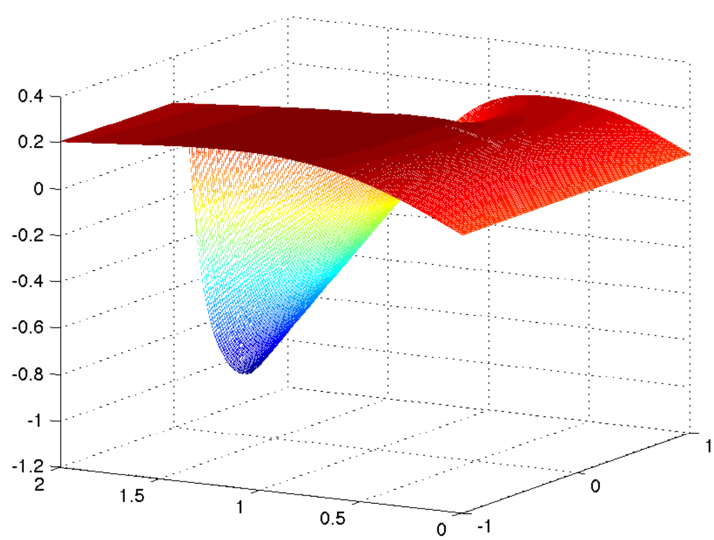

Figure 3.8: The approximation of $A(x, y)$ in $[-1, 1] \times [0, 2]$

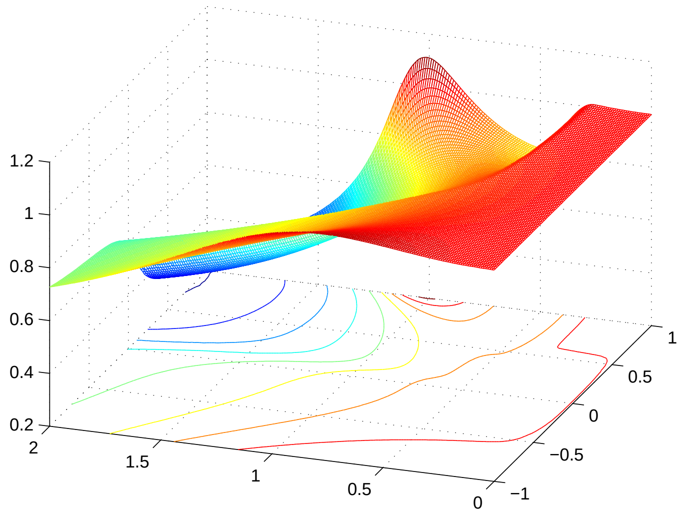

Figure 3.9: The real-part wave $Ae^{-\omega b}\cos(\omega a)$ in $[-1, 1] \times [0, 2]$

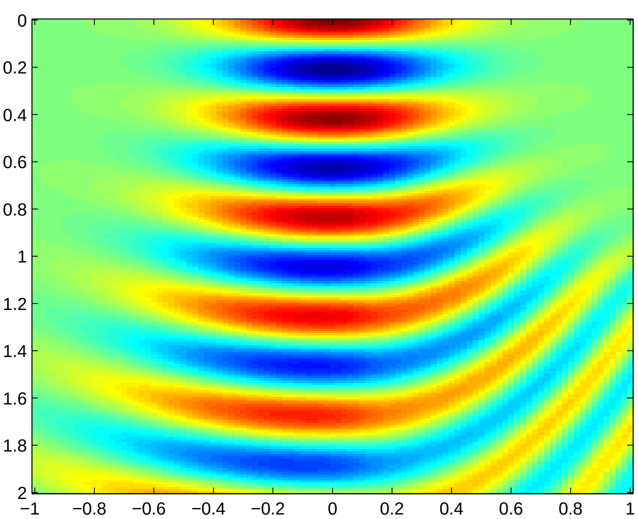

(a) Imagesc picture

Simulation in the medium C_4

C_4 is an inhomogeneous medium with $c(x,y)$ defined as

$$\begin{cases} 1 - 8[\dfrac{(x-1.02)^2}{4} + 4(y-1)^2 - \dfrac{1}{4}]^2 & \text{if } \dfrac{(x-1.02)^2}{4} + 4(y-1)^2 \le \dfrac{1}{4} \\ & \quad \text{and } x \le 1.02\,; \\ 1 - 8[4(y-1)^2 - \dfrac{1}{4}]^2 & \text{if } \dfrac{3}{4} \le y \le \dfrac{5}{4} \text{ and } x > 1.02\,; \\ 1 & \text{everywhere else.} \end{cases}$$

Figure 3.10: The medium C_4

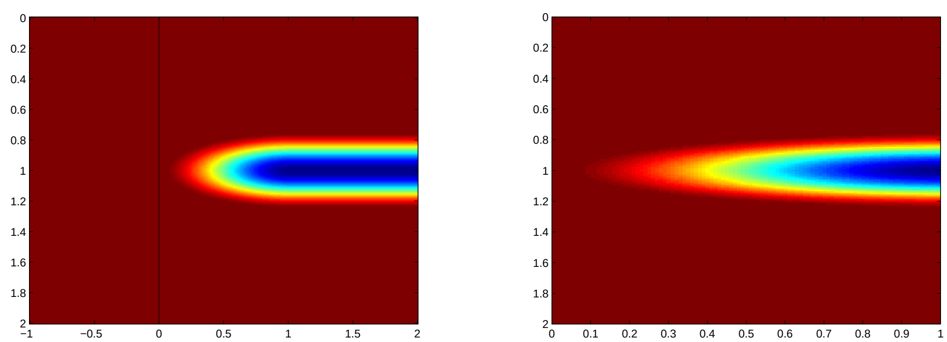

(a) Over the domain $[-1, 2] \times [0, 2]$ (b) Over the domain $[0, 1] \times [0, 2]$

Noticing that C_4 is homogeneous with $c(x,y) = 1$ in the left-half plane, we assume $d_L = d_5$ where d_5 is the approximation of $d(y)$ in the medium C_1, shown in Figure 2.7. Now we start to find d_R. We use d_5 as the initial guess for d_0 to approximate f_0. The characteristic curves for f_0 are shown below

Figure 3.11: The characteristic curves with initial points from 0.02 to 1 with $\Delta x = 0.02$ and the y coordinate restricted within $[0, 2.4]$

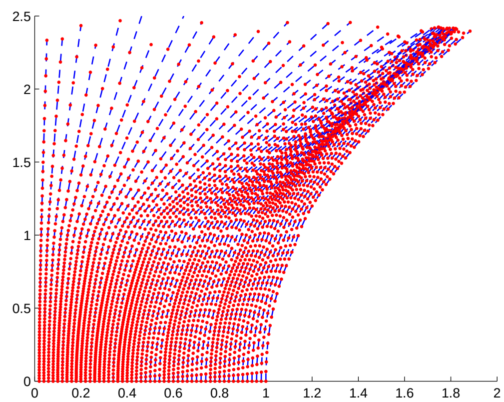

(a) Overview

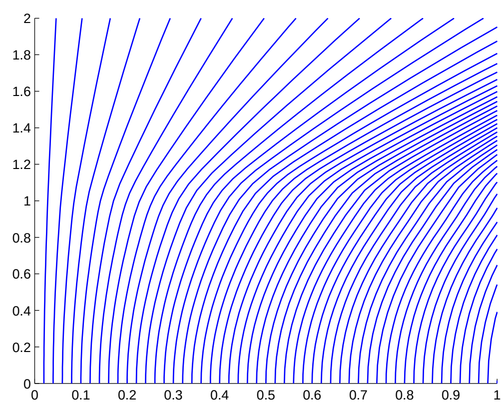

(b) Close-up in $[0, 1] \times [0, 2]$

Let $x_1 = 0.5$. We continue the iterations until $\max|d_4 - d_3|$ drops below 10^{-4}:

$$\max_{0 \le y \le 2.4} |d_1(y) - d_0(y)| = 0.0563 \qquad \max_{0 \le y \le 2.4} |d_2(y) - d_1(y)| = 0.0034$$
$$\max_{0 \le y \le 2.4} |d_3(y) - d_2(y)| = 3.07 \times 10^{-4}, \quad \max_{0 \le y \le 2.4} |d_4(y) - d_3(y)| = 1.6 \times 10^{-5}.$$

We have a comparison between d_0 and d_4

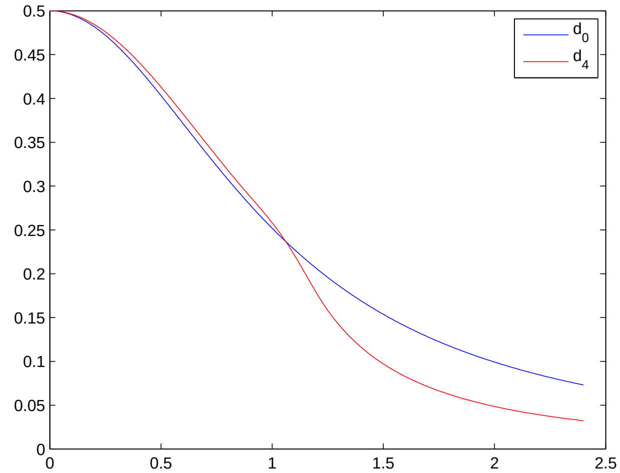

Following the steps in Section 3.2, we use d_L and d_R to approximate $f(x, y)$ in the domain $[-1, 1] \times [0.2]$

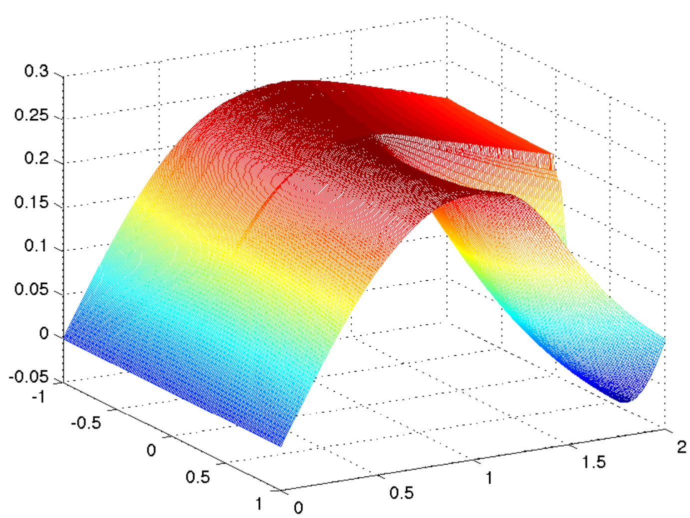

We use the approximation of $f(x, y)$ to simulate the amplitude $A(x, y)$ in the domain $[-1, 1] \times [0.2]$

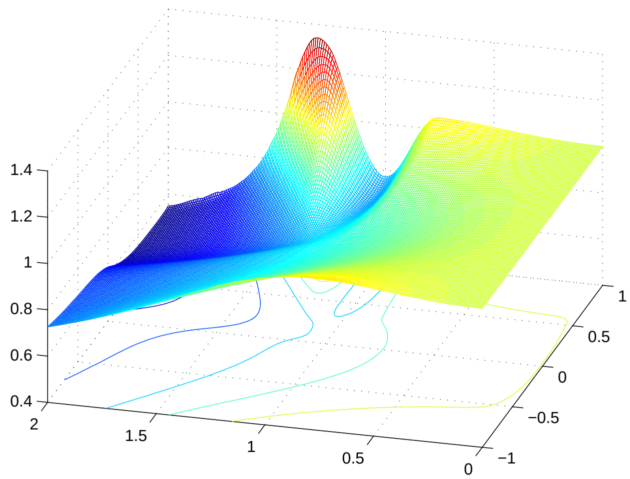

Finally, we simulate the wave and the imagesc picture of its real part $Ae^{-\omega b}cos(\omega a)$ is shown below

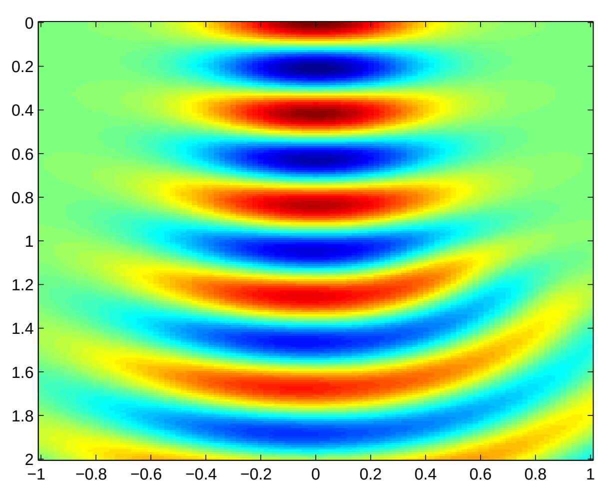

Simulation in the medium C_5

C_5 is an inhomogeneous medium with $c(x,y)$ defined as

$$\begin{cases} 1-8[\frac{(x-1.02)^4}{4}+(y-1)^2-\frac{1}{4}]^2 & \text{if } \frac{(x-1.02)^4}{4}+(y-1)^2 \le \frac{1}{4} \\ & \text{and } x \le 1.02\,; \\ 1-8[(y-1)^2-\frac{1}{4}]^2 & \text{if } \frac{1}{2} \le y \le \frac{3}{2} \text{ and } x > 1.02\,; \\ 1 & \text{everywhere else.} \end{cases}$$

Figure 3.12: The medium C_5

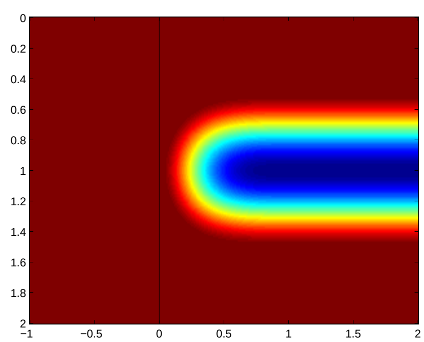

(a) Over the domain $[-1,2]\times[0,2]$

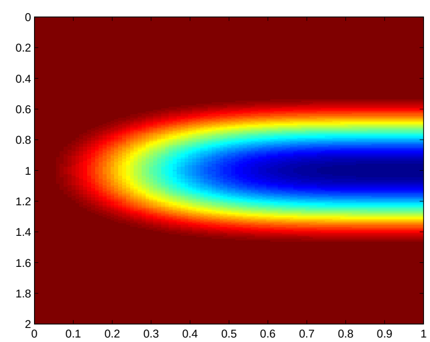

(b) Over the domain $[0,1]\times[0,2]$

Our algorithm is not applicable in this case because the characteristic curves for f_0 have intersections in the right-half domain $[0,1]\times[0,2]$ when using d_5 — the approximation of $d(y)$ in the medium C_1, shown in Figure 2.7 — as the initial guess for d_0 to approximate f_0.

Figure 3.13: The characteristic curves for f_0 with initial points from 0.02 to 1 with $\Delta x = 0.02$ and the y coordinate restricted within $[0, 2.4]$

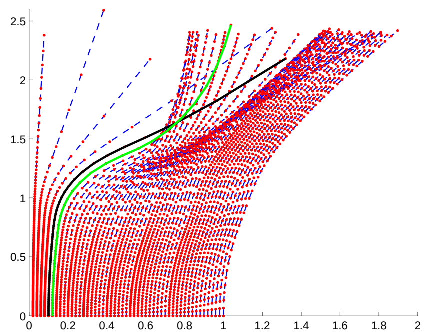

(a)

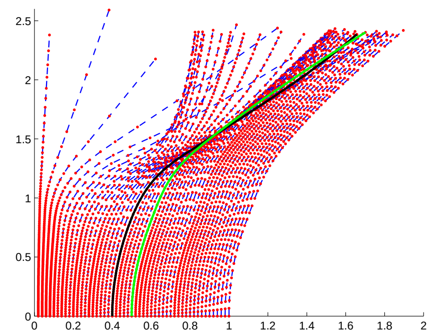

(b)

In Figure 3.13(a), the black characteristic curve with the initial point $x_0 = 0.1$ intersects the green one with the initial point $x_0 = 0.12$. In Figure 3.13(b), the black characteristic curve with the initial point $x_0 = 0.4$ intersects the green one with the initial point $x_0 = 0.5$.

Chapter 4

Comparisons between Our Model and Others

In this chapter, we compare the simulation results from our model to two other models' in several media. The first model is the Helmholtz equation with the Sommerfeld radiation condition. The second model proposes a non-iterative method for $d(y)$ and uses its approximation to simulate the wave.

4.1 Helmholtz Equation with the Sommerfeld Radiation Condition

In this section, we study the numerical solution of the Helmholtz equation with the Sommerfeld radiation condition and compare its simulation results with our model's in several media.

4.1.1 Numerical Scheme

Consider the Helmholtz equation in the lower half-plane of $\mathbb{R}^2$

$$\Delta U(x,y) + \frac{\omega^2}{c^2(x,y)} U(x,y) = 0, \quad (x,y) \in \mathbb{R}^2 \text{ and } y \leq 0 \tag{4.1}$$

with the boundary condition $U(x,0) = \exp(-\frac{\omega x^2}{2})$ on the x-axis. We assume that (4.1) is associated with the Sommerfeld radiation condition

$$\lim_{\mathbf{r}\to\infty} \mathbf{r}^{\frac{1}{2}}(\frac{\partial}{\partial \mathbf{r}}U(\mathbf{r}\hat{z}) - i\frac{\omega}{c(\mathbf{r}\hat{z})}U(\mathbf{r}\hat{z})) = 0, \text{ where } z = (x,y),\ \hat{z} = \frac{z}{|z|} \text{ and } \mathbf{r} = |z|.$$

We consider to simulate this Helmholtz equation in a rectangular domain $[-L, L] \times [0, L]$ with U satisfying

$$\frac{\partial}{\partial \mathbf{r}}U(\mathbf{r}\hat{z}) - i\frac{\omega}{c(\mathbf{r}\hat{z})}U(\mathbf{r}\hat{z}) = 0$$

on the boundaries $\{x = -L\}$, $\{y = L\}$ and $\{x = L\}$. Assume that we have the following set of grids in this rectangular domain

$$\{(x_j, y_n) \mid x_j = -L + (j-1)\Delta x,\ y_n = (n-1)\Delta y\}$$

where $j = 1, 2, \cdots, 2M+1$ with $M = L/\Delta x$, $n = 1, 2, \cdots, N+1$ with $N = L/\Delta y$ and $\Delta x = \Delta y$. We use U_j^n to denote $U(x_j, y_n)$.

The numerical scheme for this problem is given as

$$\frac{U_{j+1}^n - 2U_j^n + U_{j-1}^n}{\Delta x^2} + \frac{U_j^{n+1} - 2U_j^n + U_j^{n-1}}{\Delta y^2} + \frac{\omega^2 U_j^n}{(c_j^n)^2} = 0$$

or rearranging into

$$U_j^{n-1} + \left(\mathbf{s}U_{j+1}^n + \mathbf{t}_j^n U_j^n + \mathbf{s}U_{j-1}^n\right) + U_j^{n+1} = 0$$

$$\mathbf{s} = (\frac{\Delta y}{\Delta x})^2 \quad \mathbf{t}_j^n = (-2 - 2\mathbf{s} + (\frac{\omega \Delta y}{c_j^n})^2)$$

with the following boundary conditions

(1) When $1 \le j \le M+1$ and $n = 1$

$$U_j^1 = e^{-\frac{\omega}{2}(-L+(j-1)\Delta x)^2}.$$

(2) When $1 \le j \le M+1$ and $n = N+1$

$$(\frac{1}{\sqrt{1+\tau^2}\Delta x} - ik_j^{N+1})U_j^{N+1} + \big(\frac{\tau-1}{\sqrt{1+\tau^2}\Delta x}U_j^N - \frac{\tau}{\sqrt{1+\tau^2}\Delta x}U_{j+1}^N\big) = 0$$

where $\tau = \dfrac{M+1-j}{N}$ and $k_j^{N+1} = \dfrac{\omega}{c_j^{N+1}}$.

(3) When $M+1 < j \le 2M+1$ and $n = N+1$

$$(\frac{1}{\sqrt{1+\tau^2}\Delta x} - ik_j^{N+1})U_j^{N+1} + \big(\frac{\tau-1}{\sqrt{1+\tau^2}\Delta x}U_j^N - \frac{\tau}{\sqrt{1+\tau^2}\Delta x}U_{j-1}^N\big) = 0$$

where $\tau = \dfrac{j-M-1}{N}$ and $k_j^{N+1} = \dfrac{\omega}{c_j^{N+1}}$.

(4) When $j = 1$ and $2 \le n \le N$

$$(\frac{1}{\sqrt{1+\tau^2}\Delta x} - ik_1^n)U_1^n + \big(\frac{\tau-1}{\sqrt{1+\tau^2}\Delta x}U_2^n - \frac{\tau}{\sqrt{1+\tau^2}\Delta x}U_2^{n-1}\big) = 0$$

where $\tau = \dfrac{n-1}{M}$ and $k_1^n = \dfrac{\omega}{c_1^n}$.

(5) When $j = 2M+1$ and $2 \le n \le N$

$$(\frac{1}{\sqrt{1+\tau^2}\Delta x} - ik_{2M+1}^n)U_{2M+1}^n + \big(\frac{\tau-1}{\sqrt{1+\tau^2}\Delta x}U_{2M}^n - \frac{\tau}{\sqrt{1+\tau^2}\Delta x}U_{2M}^{n-1}\big) = 0$$

where $\tau = \dfrac{n-1}{M}$ and $k_{2M+1}^n = \dfrac{\omega}{c_{2M+1}^n}$.

4.1.2 Comparisons with Our Model

We implement this scheme to simulate the wave and denote its real part $Ae^{-\omega b}\cos(\omega a)$ by u_{HS}. The real part of the wave in our model is represented by u_{OM}. We compare u_{HS} with u_{OM} in the following media.

Figure 4.1: **Comparison in the medium** C_1

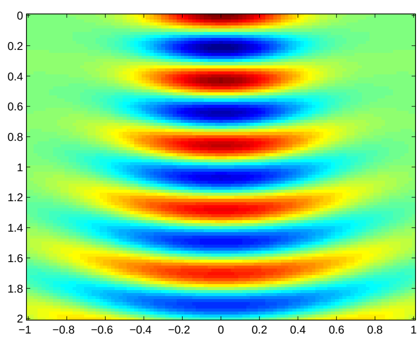

(a) u_{HS}

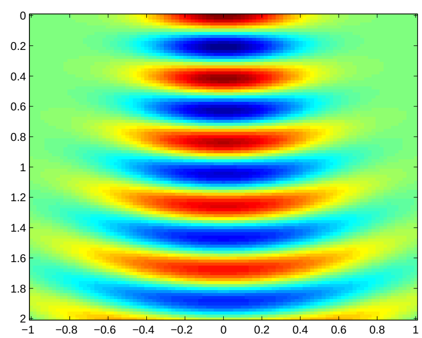

(b) u_{OM}

Figure 4.2: **Comparison in the medium** C_2

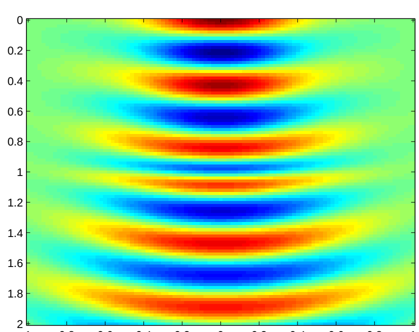

(a) u_{HS}

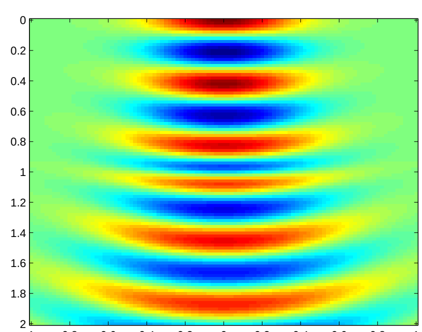

(b) u_{OM}

Figure 4.3: **Comparison in the medium C_3**

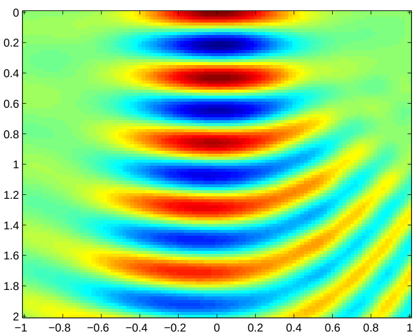

(a) u_{HS}

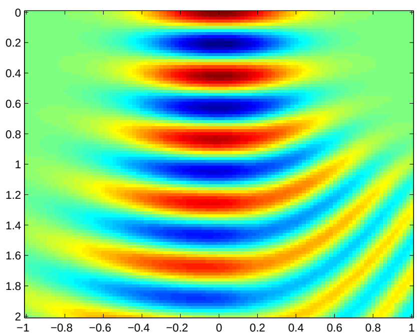

(b) u_{OM} with d_L and d_R

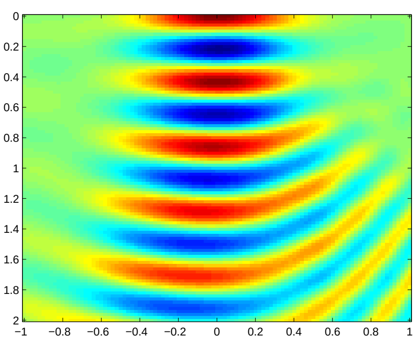

(c) u_{HS}

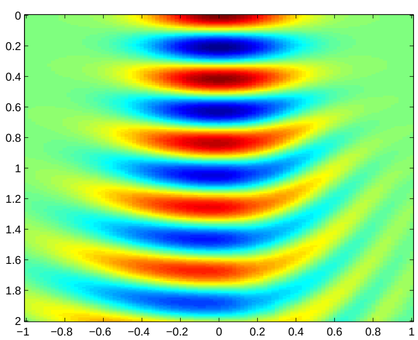

(d) u_{OM} with d_L

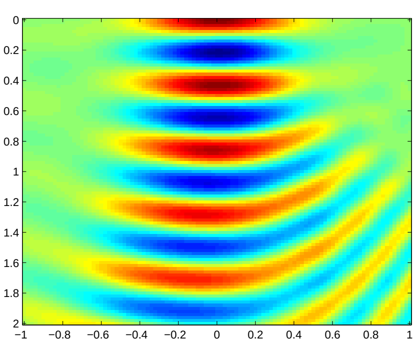

(e) u_{HS}

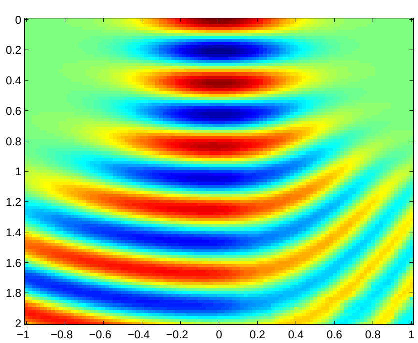

(f) u_{OM} with d_R

Remarks. In Figure 4.3, d_L represents d_5 — the approximation of $d(y)$ in the medium C_1 — shown in Figure 2.7. d_R represents d_3 — the approximation of $d(y)$ obtained in the simulation of $f(x, y)$ over the domain $[0.1, 1] \times [0, 2]$ in the medium C_3 — shown in Figure 2.18. In Figure 4.3(b), u_{OM} with d_L and d_R represents the real part of the wave whose simulation uses d_L and d_R in the left- and right-half domain respectively. In Figure 4.3(d), u_{OM} with d_L represents the real part of the wave whose simulation uses d_L in both of the left- and right-half domains. In Figure 4.3(f), u_{OM} with d_R represents the real part of the wave whose simulation uses d_R in both of the left- and right-half domains. From these three comparisons, its clear that using two different $d(y)$ in the left and right half-domain respectively delivers the closest result to the Helmholtz equation in the medium C_3.

4.2 The Wave Model with a Non-Iterative Method for $d(y)$

In this model, we derive a system of linear ordinary differential equations for $f(0, y)$ and $d(y)$ by performing the degeneracy analysis on (1.10) and (1.11). We apply the fourth order Runge-Kutta method on this system to obtain the approximations of $f(0, y)$ and $d(y)$. We use these simulation results to approximate the wave Ae^{a+ib}. We compare the simulation results with our model's in several media.

4.2.1 A Non-Iterative Method for Approximation of $d(y)$

By applying the same techniques from the derivation of (3.2) for $f(0,y)$ on (2.6), we can derive an ordinary differential equation for $d(y)$. Recall (2.6)

$$d'(y)(x^3 f_y + \frac{x}{c(x,y)}) + d(y)(2x^2 f_x + 4xf(x,y) - 2\int_0^y \frac{c_x(x,s)}{c^2(x,s)} ds) = 0.$$

Divide by x

$$d'(y)(x^2 f_y + \frac{1}{c(x,y)}) + d(y)(2x f_x + 4f(x,y) - 2\frac{\int_0^y \frac{c_x(x,s)}{c^2(x,s)} ds}{x}) = 0.$$

Let x approach 0

$$\frac{d'(y)}{c(0,y)} + d(y)(4f(0,y) - 2\lim_{x\to 0}\frac{\int_0^y \frac{c_x(x,s)}{c^2(x,s)} ds}{x}) = 0.$$

If $c(x,y)$ is C^2

$$d'(y) = -c(0,y)\big(4f(0,y) - 2\int_0^y \frac{c_{xx}(0,s)}{c^2(0,s)}\, ds\big)d(y).$$

Combining with (3.2), we have a system of linear ODEs

$$\begin{aligned} d'(y) &= -c(0,y)\big(4f(0,y) - 2\int_0^y \frac{c_{xx}(0,s)}{c^2(0,s)}\, ds\big)d(y), \\ f_y(0,y) &= 2c(0,y)\big(d^2(y) - \big(f(0,y) - \int_0^y \frac{c_{xx}(0,s)}{2c^2(0,s)}\, ds\big)^2\big). \end{aligned}$$

Moreover, if $c_{xx} = 0$ on y-axis, we have a simple version

$$d'(y) = -4c(0,y)d(y)f(0,y), \tag{4.2}$$

$$f_y(0,y) = 2c(0,y)(d^2(y) - f^2(0,y)). \tag{4.3}$$

We consider using the fourth order Runge-Kutta method to solve (4.2) and (4.3). For simplicity, we only use the simple version to show its numerical scheme which is given as follows

$$\begin{aligned} d(y_{j+1}) &= d(y_j) + \frac{\Delta y}{6}(d_{k1} + 2d_{k2} + 2d_{k3} + d_{k4}) \qquad (4.4) \\ f(0, y_{j+1}) &= f(0, y_j) + \frac{\Delta y}{6}(f_{k1} + 2f_{k2} + 2f_{k3} + f_{k4}) \qquad (4.5) \end{aligned}$$

where $\{(0, y_j)\}$ is a set of equally spaced grids with spacing Δy on the y-axis and

$$\begin{aligned} d_{k1} &= -4c(0, y_j)f(0, y_j)d(y_j) \\ f_{k1} &= 2c(0, y_j)(d^2(y_j) - f^2(0, y_j)) \\ d_{k2} &= -4c(0, y_j + \frac{\Delta y}{2})(f(0, y_j) + \frac{\Delta y}{2}f_{k1})(d(y_j) + \frac{\Delta y}{2}d_{k1}) \\ f_{k2} &= 2c(0, y_j + \frac{\Delta y}{2})((d(y_j) + \frac{\Delta y}{2}d_{k1})^2 - (f(0, y_j) + \frac{\Delta y}{2}f_{k1})^2) \\ d_{k3} &= -4c(0, y_j + \frac{\Delta y}{2})(f(0, y_j) + \frac{\Delta y}{2}f_{k2})(d(y_j) + \frac{\Delta y}{2}d_{k2}) \\ f_{k3} &= 2c(0, y_j + \frac{\Delta y}{2})((d(y_j) + \frac{\Delta y}{2}d_{k2})^2 - (f(0, y_j) + \frac{\Delta y}{2}f_{k2})^2) \\ d_{k4} &= -4c(0, y_j + \Delta y)(f(0, y_j) + \Delta y f_{k3})(d(y_j) + \Delta y d_{k3}) \\ f_{k4} &= 2c(0, y_j + \Delta y)((d(y_j) + \Delta y d_{k3})^2 - (f(0, y_j) + \Delta y f_{k3})^2)\,. \end{aligned}$$

Simultaneously, we obtain the approximation of $f_y(0, y_j)$

$$f_y(0, y_j) = 2c(0, y_j)(\, d^2(y_j) - f^2(0, y_j)\,)\,.$$

4.2.2 Modeling and its Numerical Approxiation

To simulate the wave with $d(y)$ obtained by this non-iterative method, we need to revise certain steps in the approximation of $f(x, y)$ but the approximations of amplitude and wave remain the same. We take the following steps to approximate $f(x, y)$ in the domain $[-1, 1] \times [0, 2]$.

Step 1. Use $d(y)$ to calculate all the characteristics of $f(x, y)$ with initial points from -1 to -0.02 and from 0.02 to 1 with 0.02 spacing. We denote these characteristics by $\{x_r,\ y_r,\ z_r,\ p_{1r},\ p_{2r}\}$ with positive counting index $r = 1, 2, 3$ etc.

Step 2. Find subsets $S_L, S_R \subset \mathbb{N}^+$ such that (x_l, y_l) with $l \in S_L$ is the characteristic curve with initial point $x_0 = -0.02$; (x_r, y_r) with $r \in S_R$ is the characteristic curve with initial point $x_0 = 0.02$. For each grid $(0, y_j)$, we find the three nearest points to it, namely (x_{n1}, y_{n1}), (x_{n2}, y_{n2}) and (x_{n3}, y_{n3}), from the set of $\{(x_k, y_k),\ k \in S_L \cup S_R\}$ and do the linear interpolation on $(x_{n1}, y_{n1}, p_{1_{n1}})$, $(x_{n2}, y_{n2}, p_{1_{n2}})$ and $(x_{n3}, y_{n3}, p_{1_{n3}})$ to obtain the approximation of $f_x(0, y_j)$.

Step 3. At each grid (x_j, y_n) with $x_j \neq 0$, we repeat the same steps in Subsubsection 2.3.1.2 to approximate $f(x_j, y_n)$, $f_x(x_j, y_n)$ and $f_y(x_j, y_n)$ from the characteristic set — the union of $\{x_r, y_r, z_r, p_{1r}, p_{2r}\}$ and $\{0, y_j, f(0, y_j), f_x(0, y_j), f_y(0, y_j)\}$.

4.2.3 Comparisons with Our Model

We will compare the approximations of $d(y)$ obtained by this non-iterative method, $f(x, y)$, the amplitude and the real part of the wave with our model's in several media.

Comparisons in the medium C_1

We use d to denote the approximation of $d(y)$ obtained by this non-iterative method. We compare it with various d_5 from Sub-subsection 2.3.3.1.

Figure 4.4: Comparisons between d and d_5 with different x_1

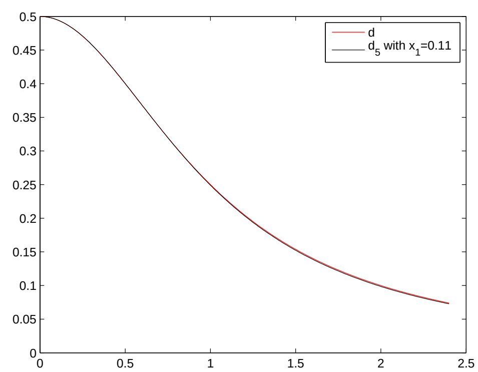

(a) $\max\limits_{y\in[0,2.4]} |d - d_5| = 0.0015$

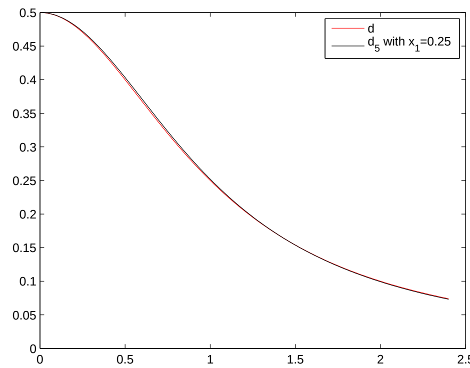

(b) $\max\limits_{y\in[0,2.4]} |d - d_5| = 0.0035$

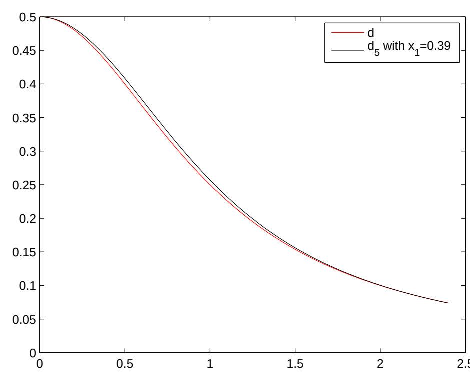

(c) $\max\limits_{y\in[0,2.4]} |d - d_5| = 0.0094$

Figure 4.4 shows that there is not much difference between d and d_5 with $x_1 = 0.11$, 0.25 and 0.39. This implies that there should be not much difference between $f(x, y)$, the amplitude $A(x, y)$ and the real part of the wave $Ae^{-\omega b}cos(\omega a)$ with these two models. The following comparisons verify this claim.

Figure 4.5: Comparisons of $f(x, y)$

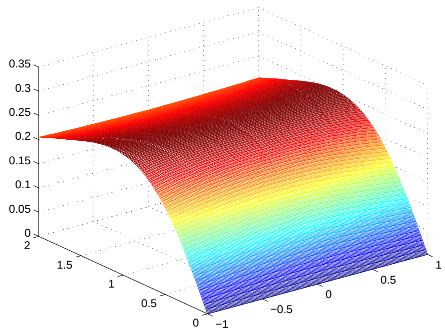

(a) An overview picture of $f(x, y)$ simulated with d

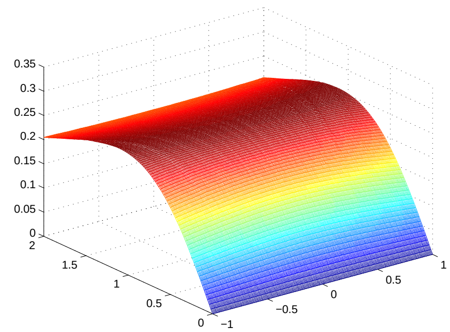

(b) An overview picture of $f(x, y)$ simulated with d_5

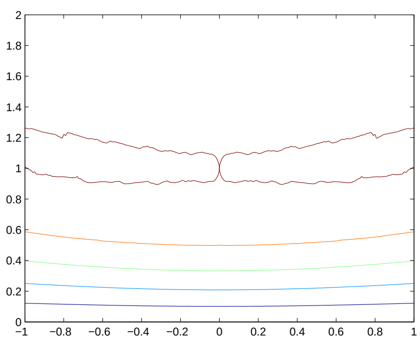

(c) A contour picture of $f(x, y)$ simulated with d

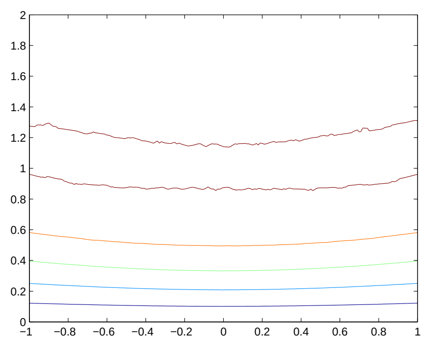

(d) A contour picture of $f(x, y)$ simulated with d_5

Figure 4.6: Comparisons of $A(x, y)$

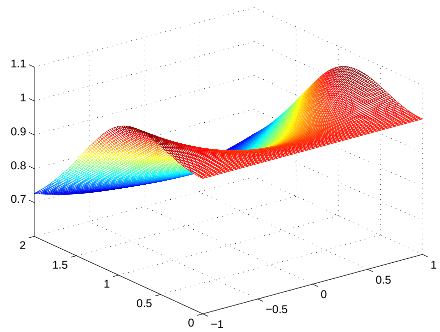

(a) An overview picture of $A(x, y)$ simulated with d

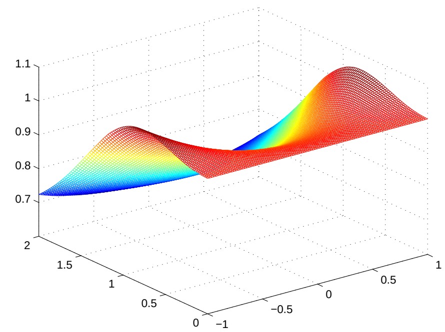

(b) An overview picture of $A(x, y)$ simulated with d_5

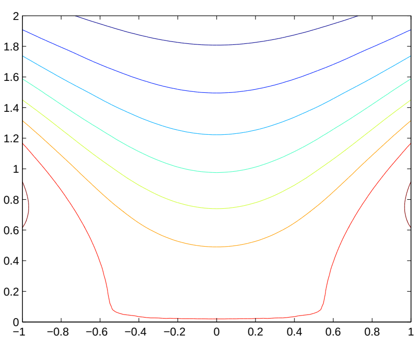

(c) A contour picture of $A(x, y)$ simulated with d

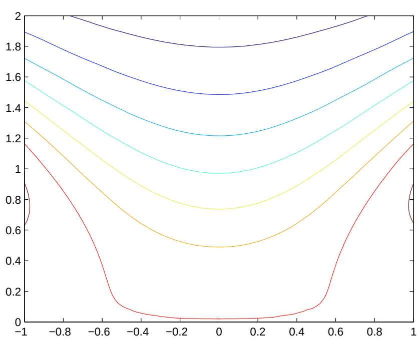

(d) A contour picture of $A(x, y)$ simulated with d_5

Figure 4.7: Comparison of $Ae^{-\omega b}cos(\omega a)$

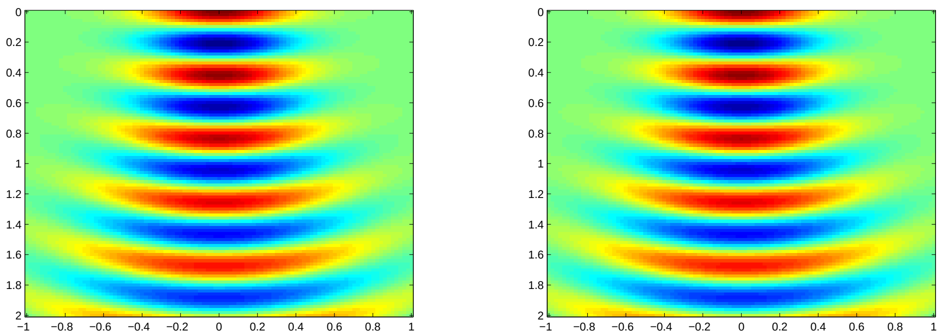

(a) An imagesc picture of the real-part wave simulated with d

(b) An imagesc picture of the real-part wave simulated with d_5

where all the simulations in our model are done with $d_5(x_1 = 0.25)$.

Remarks. There is not much difference between d and $d_5(x_1 = 0.25)$, and in the simulation results of the real part of the wave between these two models. If we use $d(y)$ obtained by this non-iterative method to simulate the wave in the whole domain $[-1, 1] \times [0, 2]$ in the medium C_3, we expect u_{OM} to have similar results as shown in Figure 4.3(d). Due to the large difference exhibited between Figure 4.3(c) and 4.3(d), we suggest using this wave model in media where $c(x, y)$ does not depend on x.

Comparisons in the medium C_2

We use d to denote the approximation of $d(y)$ obtained by the non-iterative method. We compare it with various d_4 from Sub-subsection 2.3.3.2.

Figure 4.8: Comparisons between d and d_4 with different x_1

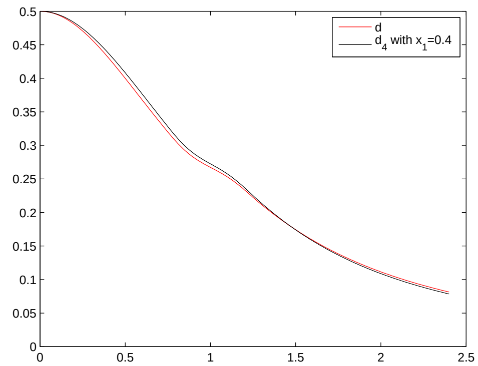

(a) $\max_{y\in[0,2.4]} |d - d_4| = 0.0088$

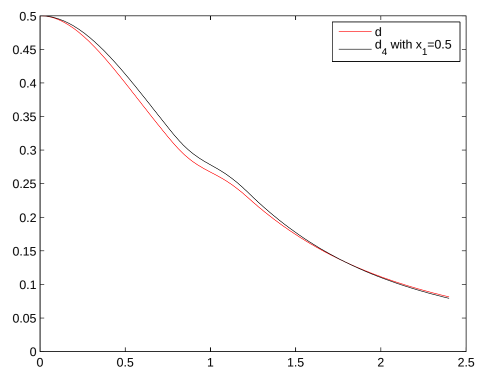

(b) $\max_{y\in[0,2.4]} |d - d_4| = 0.0146$

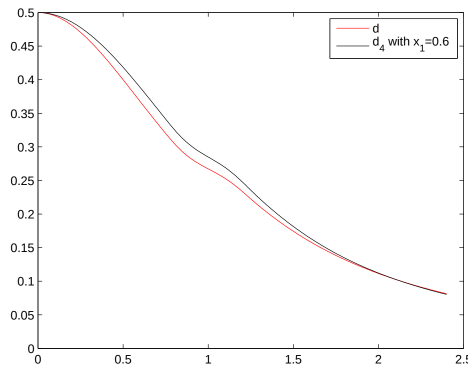

(c) $\max_{y\in[0,2.4]} |d - d_4| = 0.0216$

Figure 4.8 shows that there are visible differences between d and d_4 with $x_1 = 0.4$, 0.5 and 0.6, and the maximum difference becomes larger when x_1 is farther away from the y-axis. Next, we compare $f(x, y)$, the amplitude $A(x, y)$ and the real part of the wave $Ae^{-\omega b}cos(\omega a)$ simulated with d to those simulated with $d_4(x_1 = 0.5)$ in our model.

Figure 4.9: Comparisons of $f(x, y)$

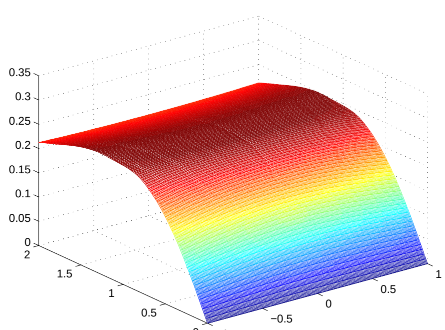

(a) An overview picture of $f(x, y)$ simulated with d

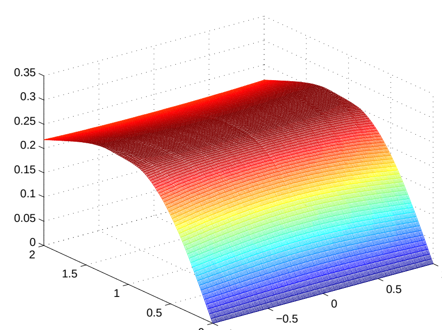

(b) An overview picture of $f(x, y)$ simulated with d_4

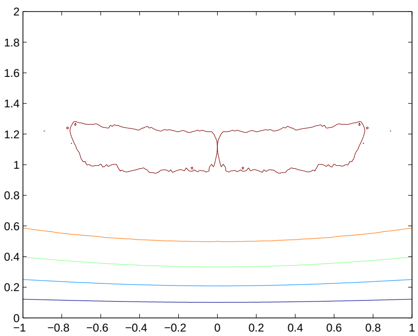

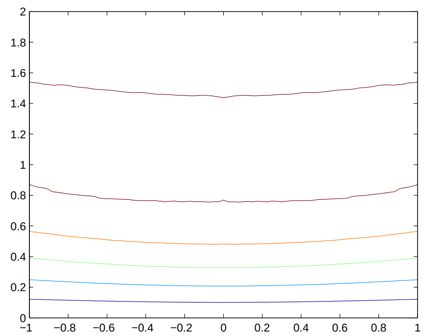

(c) A contour picture of $f(x, y)$ simulated with d

(d) A contour picture of $f(x, y)$ simulated with d_4

Figure 4.10: Comparisons of $A(x, y)$

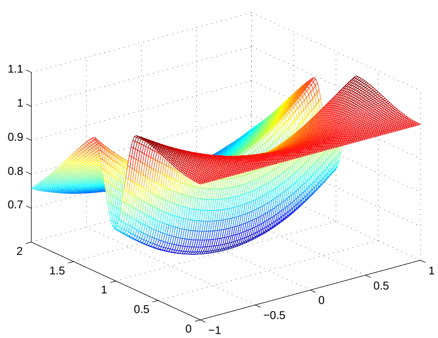

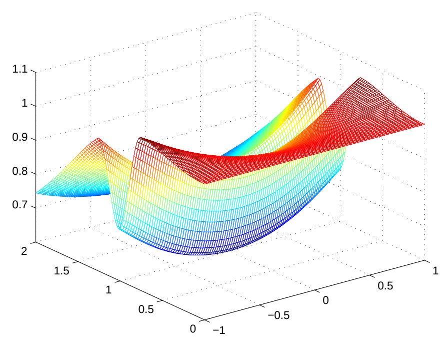

(a) An overview picture of $A(x, y)$ simulated with d

(b) An overview picture of $A(x, y)$ simulated with d_4

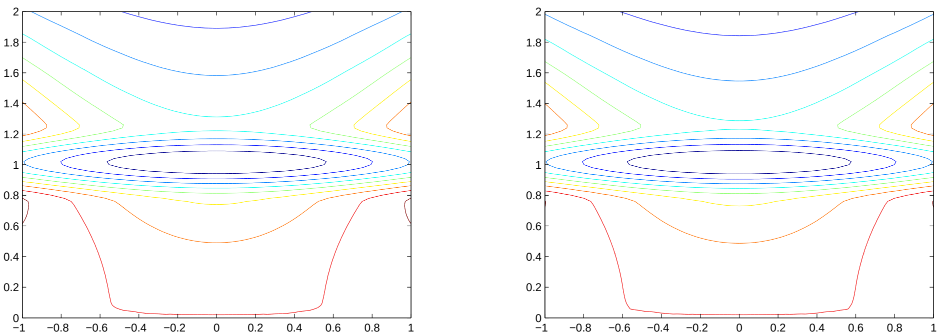

(c) A contour picture of $A(x,y)$ simulated with d

(d) A contour picture of $A(x,y)$ simulated with d_4

Figure 4.11: Comparison of $Ae^{-\omega b}cos(\omega a)$

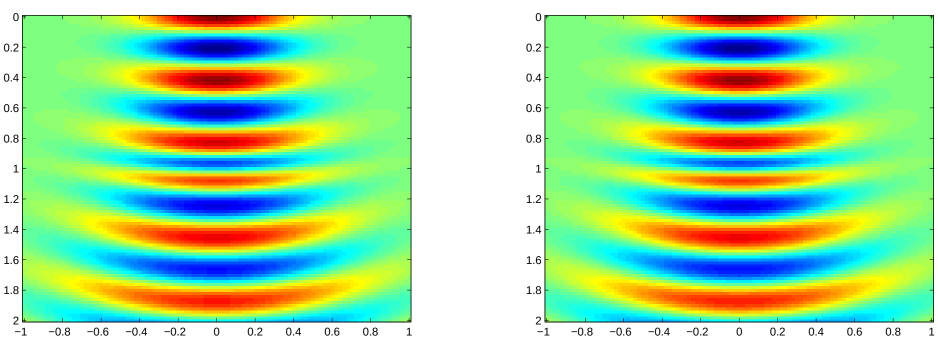

(a) An imagesc picture of the real-part wave simulated with d

(b) An imagesc picture of the real-part wave simulated with d_4

4.3 Future Research

The results presented in this thesis can be extended in different directions. It would, for example, be natural to consider the 3D complex eikonal equation and see if a similar approximate model based on a coupled system of ordinary and partial differential equations could be developed.

Higher order approximations both in the continuous system and in the numerical approximations could be explored. This could be done first in the 2D case, and if a satisfactory 3D theory can been developed, higher order approximations could also be extended to 3D. For the continuous approximation, the current model for the imaginary part of the solution of the complex eikonal equation is based on the function d(y). This could be extended to more than one function where each such function would be defined by an ordinary differential equation. In the numerical approximations, higher order schemes for the ordinary and partial differential equations should be quite straightforward.

Our focus has been to establish a proof of concept, and therefore the velocity profiles in the numerical examples have been chosen such that the central ray is straight and coincides with the y-axes. In general this ray is curved as in Gaussian beam ray tracing. The partial differential equations in our model would then have to be solved in a transformed coordinate system. This generalization is necessary if more realistic applications should be tackled.

Bibliography

[1] V.M. Babich and M.M. Popov, Gaussian summation method, Radiophysics and Quantum Electronics 32 (1989), 1063-1081.

[2] M. Bardi, M.G. Crandall, L.C. Evans, H.M. Soner and P.E. Souganidis, Viscosity solutions and applications, Springer, Berlin, 1997.

[3] Garrett Birkhoff and Gian-Carlo Rota, Ordinary differential equations, John Wiley and Sons, New York, 1989.

[4] N. Bleistein, Mathematical methods for wave phenomena, Academic Press, Orlando, Florida, 1984.

[5] N. Bleistein, J.K. Cohen and John W. Jr. Stockwell, Mathematics of multidimensional seismic imaging, migration, and inversion, Springer-Verlag, New York, 2001.

[6] N. Bleistein, Mathematics of modeling, migration and inversion with Gaussian beams, preprint (2008), available at `http://www.cwp.mines.edu/~norm/`.

[7] V. Červený, Expansion of a plane wave into Gaussian beams, Studia Geoph. et Geod. 26 (1982), 120-131.

[8] V. Červený, Gaussian beam synthetic seismograms, J. Geophys. 58 (1985), 44-72.

[9] V. Červený, Seismic ray theory, Cambridge University Press, Cambridge, 2001.

[10] V. Červený, L. Klimeš and and I. Pšenčik, Paraxial ray approximation in the computation of seismic wave fields in inhomogeneous media, Geo. J. R. Astr. Soc. 79 (1984), 89-104.

[11] V. Červený, L. Klimeš and and I. Pšenčik, Seismic ray method: recent developments: Chapter 1, Advances in Geophysics 48 (2007), 1-126.

[12] V. Červený, M.M. Popov and I. Pšenčik, Computation of wave fields in inhomogeneous media — Gaussian beam approach, Geo. J. R. Astr. Soc. 70 (1982), 109-128.

[13] J.F. Claerbout, Imaging the earth's interior, Blackwell Scientific Publications, Oxford, 1985.

[14] J.F. Claerbout, The simplest gaussian beam, preprint, SEP-28, available at `http://sepwww.stanford.edu/theses/sep28/28_13_abs.html`.

[15] B. Engquist and O. Runborg, Computational high frequency wave propagation, Acta Numerica 12 (2003), 181-266.

[16] L.C. Evans, Partial Differential Equations, American Mathematical Society, Providence, Rhode Island, 1998.

[17] D. Gilbarg and N.S. Trudinger, Elliptic Partial Differential Equations of Second Order, Springer, Berlin, 2001.

[18] N.R. Hill, Gaussian beam migration, Geophysics 55 (1990), 1416-1428.

[19] N.R. Hill, Prestack Gaussian-beam depth migration, Geophysics 66 (2001), 1240-1250.

[20] S. Li, S. Fomel and A. Vladimirsky, Improving wave-equation fidelity of Gaussian beams by solving the complex eikonal equation, 2011 SEG Annual Meeting, San Antonio, Texas, 2011.

[21] R. Magnanini and G. Talenti, On complex-valued solutions to a 2-D eikonal equation. Part one: qualitative properties, Contemporary Math. 238 (1999), 203-229.

[22] R. Magnanini and G. Talenti, On complex-valued solutions to a 2-D eikonal equation. Part two: existence theorems, SIAM J. Math. Anal. 34 (2002), 805-835.

[23] R. Magnanini and G. Talenti, On complex-valued solutions to a 2D eikonal equation. Part three: analysis of a Bäcklund transformation, Applicable Analysis 85 (2006), 249-276.

[24] R. Magnanini and G. Talenti, On complex-valued solutions to a 2D eikonal equation. Part four: continuation past a caustic, Milan J. Math. (2009), 1-66.

[25] R.L. Nowack, Calculation of synthetic seismograms with Gaussian beams, Pure and Applied Geophysics 160 (2003), 487-507.

[26] M.M. Popov, A new method of computation of wave fields using Gaussian beams, Wave Motion 4 (1982), 85-97.

[27] M.M. Popov, Ray theory and gaussian beam method for geophysicists, EDUFBA, Salvador, Brazil, 2002.

[28] M.M. Popov and I. Pšenčik, Computation of ray amplitudes in inhomogeneous media with curved interfaces, Studia Geoph. et Geod. 222 (1978), 248-258.

[29] N.M. Tanushev, Superpositions and higher-order Gaussian beams, Communications in Mathematical Sciences 6 (2008), 449-475.